UNIVERSIDADE ESTADUAL PAULISTA
"JÚLIO DE MESQUITA FILHO"
Câmpus de São José do Rio Preto

Bianca Gottardo de Almeida

Nanomateriais híbridos contendo prata e óxido de grafeno reduzido para atividade antifúngica

São José do Rio Preto
2022

Bianca Gottardo de Almeida

Nanomateriais híbridos contendo prata e óxido de grafeno reduzido para atividade antifúngica

Tese apresentada como parte dos requisitos para obtenção do título de Doutor em Microbiologia, junto ao Programa de Pós-Graduação Microbiologia, do Instituto de Biociências, Letras e Ciências Exatas da Universidade Estadual Paulista “Júlio de Mesquita Filho”, Câmpus de São José do Rio Preto.

Financiadora: CAPES

Orientador: Profª. Drª. Diogo Paschoalini Volanti

São José do Rio Preto
2022

G685n

Gottardo, Bianca
Nanomateriais híbridos contendo prata e óxido de grafeno reduzido para atividade antifúngica / Bianca Gottardo. -- São José do Rio Preto, 2022
57 p. : il., tabs.

Tese (doutorado) - Universidade Estadual Paulista (Unesp), Instituto de Biociências Letras e Ciências Exatas, São José do Rio Preto
Orientador: Diogo Paschoalini Volanti

1. Dermatomicoses. 2. Óxido de grafeno reduzido. 3. Nanopartículas de prata. 4. Antifúngico. I. Título.

Sistema de geração automática de fichas catalográficas da Unesp. Biblioteca do Instituto de Biociências Letras e Ciências Exatas, São José do Rio Preto. Dados fornecidos pelo autor(a).
Essa ficha não pode ser modificada.

Bianca Gottardo de Almeida

Nanomateriais híbridos contendo prata e óxido de grafeno reduzido para atividade antifúngica

Tese apresentada como parte dos requisitos para obtenção do título de Doutor em Microbiologia junto ao Programa de Pós-Graduação em Microbiologia, do Instituto de Biociências, Letras e Ciências Exatas da Universidade Estadual Paulista “Júlio de Mesquita Filho”, Câmpus de São José do Rio Preto.

Financiadora: CAPES

Comissão Examinadora

Prof. Dr. Diogo Paschoalini Volanti
UNESP – Câmpus de São José do Rio Preto
Orientador

Profª. Drª. Maria Lúcia Scroferneker
UFRGS - Porto Alegre

Prof. Dr. João Roberto Antônio
FAMERP - São José do Rio Preto

Prof. Dr João Paulo Zen Siqueira
FAMERP – São José do Rio Preto

Profª. Drª Elza Maria Castilho
FAMERP- São José do Rio Preto

São José do Rio Preto
31 de março de 2022

AGRADECIMENTOS

Aos meus pais e irmãos por me incentivarem sempre e não me deixarem desistir quando quis, pois sabiam que eu estava dentro do meu maior sonho; e estarem sempre presentes como meu escudo emocional e espiritual.

Aos meus avós maternos e paternos por me darem os melhores e sábios conselhos sobre vida os quais sempre vou lembrar, mesmo não estando presentes fisicamente: Vó Nilde e Vó Chicão; Vó Alzira e Vó Odair.

Ao meu noivo Breno Sampaio por mostrar sempre com clareza os melhores passos e decisões a seguir.

Aos tios e primos da família Gottardo e Almeida por sempre me colocarem pra cima e apoiarem as minhas escolhas.

Às minhas amigas Awdrey Canhoto, Isabela Calijuri, Maria Eduarda Mendonça, Maria Laura Lourenço, Nina Morita, Victoria Tavares, pelas risadas, abraços e palavras que me fortaleceram sempre.

Ao meu orientador por me apoiar, ensinar e pela parceria durante os anos de mestrado e doutorado.

Aos amigos e parceiros de trabalho do Laboratório de Microbiologia da Faculdade de Medicina de São José do Rio Preto: Thiago Lemes, Taíza Maschio, Mariela Ribeiro, Letícia Mozaner, Natália Seron Brizzoti, Maicon Henrique Caetano, Emilia Gianizella, Luceli Souza e Professora Zêmia; e amigos e parceiros do Laboratório de Materiais e Sustentabilidade-LABMATSUS da UNESP: Tarcísio Perfecto, Andreza Zoccal e Vinícius Lopes.

Aos membros titulares e suplentes por terem aceito o convite de participação e contribuírem com seus ricos conhecimentos.

O presente trabalho foi realizado com apoio da Coordenação de Aperfeiçoamento de Pessoal de Nível Superior - Brasil (CAPES) - Código de Financiamento 001, à qual agradeço durante esses 3 anos.

RESUMO

As infecções superficiais de cabelo, pele ou unhas, frequentemente causadas por fungos, são reportadas por pacientes em clínicas dermatológicas. Além do impacto estético, dor, prurido, deformidade ungueal e tecidual, podem ser fonte de entrada para outros patógenos primários ou oportunistas alcançando tecidos mais profundos. O alto custo do tratamento, a toxicidade e surgimento de patógenos resistentes justificam a busca por novas drogas. Sendo assim, o objetivo deste estudo foi avaliar a atividade antifúngica de nanocompósitos (NCs) de óxido de grafeno reduzido e prata (rGO/Ag) contra isolados clínicos de microrganismos pertencentes ao laboratório de Microbiologia da Faculdade de Medicina de São José de São José do Rio Preto. As NCs foram caracterizadas por análise de difração de raios X, e a morfologia e caracterização do nanocompósito, foram investigadas por microscopia eletrônica de transmissão. O ensaio de suscetibilidade antifúngica foi realizado pelo método de microdiluição seguindo o protocolo CLSI, com modificações. O perfil toxicológico foi testado em modelo *in vivo.* As nanopartículas híbridas apresentaram grande potencial inibitório frente às cepas clínicas, sem toxicidade. Este estudo fornece nova estratégia terapêutica alternativa para o controle de dermatomicoses.

Palavras–chave: Dermatomicoses. Óxido de grafeno reduzido. Nanopartículas de prata. Antifúngico.

ABSTRACT

Superficial infections of hair, skin or nails, mainly caused by fungi, are often reported by patients in dermatology clinics. In addition to the esthetic impact, itching, pain, nail and tissue deformity, can be a source of entry for other opportunistic or primary pathogens, covering more itchy tissues. The high cost of treatment, toxicity and emergence of resistant pathogens justify the search for new drugs. The aim of this study was to evaluate the antimicrobial activity of reduced graphene oxide (rGO/Ag) and silver nanocomposites (NCs) against microrganisms clinically isolated belonging to the Microbiology Laboratory of the Faculty of Medicine of São José do Rio Preto - FAMERP. The NCs were characterized by X-ray diffraction analysis, and the morphology and characterization of the nanocomposite were investigated by transmission electron microscopy. The antifungal susceptibility assay was performed by the microdilution method based on the CLSI protocol, with modifications. The toxicological profile was tested *in vivo* model. The hybrid nanoparticles showed great inhibitory effect against all clinical tested strains, without toxicity. In summary this study provides a new alternative therapeutic strategy for the control of dermatomycoses.

Keywords: Dermatomycoses. Reduced graphene oxide. Silver nanoparticles. Antifungal.

LISTA DE ILUSTRAÇÕES

LISTA DE TABELAS

LISTA DE ABREVIATURAS E SIGLAS

Ag	Silver
CA1	*Candida albicans*
CIM	Concentração inibitória mínima
COD	Crystallography open database
CLSI	Clinical laboratory standard institute
CP1	*Candida parapsilosis*
Cu	Copper
DMSO	Dimethyl sulfoxide
XRD	X-ray diffraction
EF1	*Epidermophyton floccosum* 1
EF2	*Epidermophyton floccosum* 2
GO	Graphene oxide
HRTEM	High resolution transmission electron microscopy
MC1	*Microsporum canis* 1
MC2	*Microsporum canis* 2
MIC	Minimum inhibitory concentration
NCs	Nanocomposites
NPs	Nanoparticles
PBS	Phosphate buffered saline
QAC	Quaternary ammonium compound
rGO	Reduced graphene oxide
RPM	Rotations per minute
RPMI	Roswell park memorial institute
SAED	Selected area electron diffraction

SB Sabouraud broth

SDS Sodium borohydride

STEM Screaning transmission electron microscopy

TM1 *Trichophyton mentagrophytes* 1

TM2 *Trichophyton mentagrophytes* 2

TR1 *Trichophyton rubrum* 1

TR2 *Trichophyton rubrum* 2

SUMÁRIO

1 INTRODUÇÃO E REVISÃO BIBLIOGRÁFICA

Dermatomicose é a doença fúngica de maior ocorrência entre seres humanos e animais. Estudos epidemiológicos sobre infecções fúngicas comprovam o impacto para a saúde pública mundial, dada a cura dificultada e alta disseminação dos agentes etiológicos (MOCHIZUKI *et al.*, 2020). Vários motivos são aventados para explicar o aumento da incidência de micoses em humanos: doenças crônicas, como diabetes mellitus, doença arterial periférica, imunossupressão de diversas origens (HIV ou às drogas imunossupressoras) além do uso abusivo de antibióticos (SCRAVONI; GRZONA, 2021). Os padrões elevados de temperatura e umidade, típicos das regiões tropicais, favorecem a reprodução e disseminação dos fúngicos, e nestes ambientes, a distribuição de diferentes espécies está condicionada à adaptação dos agentes ao meio ambiente, deslocamentos humanos, convívio com animais domésticos e aspectos socioeconômicos (GINTER-HANSELMAYER; NENOFF, 2019).

Diversas áreas do corpo podem expressar aspectos clínicos variados de infecções fúngicas, sendo habitualmente denominados como tinea unguium, corporis, capitis, manum, pedis e cruris. Estas lesões ocorrem conforme a área de contato primário do fungo com o hospedeiro, após trauma ou contato direto com o agente. Valorizando-se a carga fúngica, a espécie e as condições clínicas do homem, os sintomas podem ser típicos e como queixas comuns, a coceira, ardência e até dor (GRANINGER; DIAB-ELSCHAHAWI; PRESTERL, 2019). Ainda, como principais sinais são considerados: as descamações, infiltrações com abscessos, pústulas, crostas, cabelos quebradiços ou de queda fácil, e para as unhas, acometimentos, distal lateral para proximal, hiperqueratose subungueal e/ou hipertrofia(GNAT; ŁAGOWSKI; NOWAKIEWICZ, 2020).

Os dermatófitos, representam o grupo de fungos hialinos patogênicos de maior ocorrência nas doenças fúngicas superficiais, sendo que as espécies de *Epidermophyton* spp*, Microsporum* spp, *Trichophyton* spp, são as mais comuns. No entanto, mais recentemente, a partir de estudos com biologia molecular, houve a inclusão de novos gêneros, como *Arthroderma, Nannizzia, Lophophyton*, e *Paraphyton* (BEGUM *et al.*, 2020; MARTINEZ-ROSSI *et al.*, 2021), que certamente estarão enriquecendo a etiologia de infecções fúngicas superficiais conforme recursos diagnósticos aprimorados.

Outros agentes não dermatófitos, como espécies de *Candida*, *Scytalidium* e *Fusarium*, não menos importantes, têm sido considerados patógenos em diversos nichos anatômicos (RODRIGUES *et al.*, 2022). Ocorrências dermatológicas bastante comuns incluem às produzidas por espécies de *Candida*, com destaque à *Candida albicans, Candida parapsilosis* complex e *Candida krusei*, em associação a altas taxas de morbidade e mortalidade (PAPPAS *et al.*, 2018; WHALEY *et al.*, 2017).

Várias espécies de fungos, prevalentes nas micoses superficiais, apresentam fatores de virulência, enzimas e toxinas, cuja ação sobre tecido queratinizado leva a alterações estruturais importantes na pele e anexos (CHINNAPUN, 2015). Neste sentido, e como exemplo, os fungos produzem fosfolipases, proteases e outras toxinas, alterando substratos específicos, presentes nos tecidos queratinizados e, por consequência, invadem áreas adjacentes mais profundas do corpo (GUPTA; VENKATARAMAN, 2021). No entanto, mesmo que algumas espécies não possuam fatores de virulência, elas podem causar infecções fúngicas, como agentes oportunistas (SANTOS *et al.*, 2018).

Considerando as características fisiológicas e metabólicas dos fungos, tem-se a reprodução como um processo lento, e, por consequência, a identificação laboratorial por cultura também é lenta. Procurando atender aos recursos clínicos para cura de infecções por fungos, o médico opta por oferecer tratamento empírico, o que leva ao insucesso terapêutico (LIPNER; SCHER, 2019). Com os avanços tecnológicos, hoje é possível melhorar os protocolos da prática clínica, conhecendo o agente e sua resposta fenotípica aos antifúngicos, tanto espécies de leveduras quanto fungos filamentosos. De fato, relatos científicos prévios comprovam a tendência à resistência, observando-se os valores maiores de concentração inibitória mínima (CIM) (RIDZUAN *et al.*, 2019).

Tendo em vista a permanência de fungos no estrato córneo e granuloso, áreas constituintes do tecido epitelial, a maioria das opções terapêuticas considera o fármaco de aplicação tópica, ou seja, há recomendação de pomadas ou cremes contendo antifúngico (MOCHIZUKI *et al.*, 2020). No entanto, nos casos de lesões superficiais extensas ou, em micose na unha ou no couro cabeludo mais complexas, há necessidade de adoção de antifúngicos orais, em comprimido. Embora haja uma variedade de classe de fármacos para tratamento de doenças fúngicas superficiais, a terbinafina, e os derivados azólicos, fluconazol e itraconazol, são os poucos compostos de maior escolha médica(GUPTA; VENKATARAMAN, 2021).

Os efeitos colaterais dos antifúngicos são observados especialmente quando aplicados por tempo prolongado, acarretando graves prejuízos aos tecidos hepático e renal (KABLY *et al.*, 2022). Além dos efeitos adversos das drogas, à não adesão ao tratamento pelo paciente dificulta a melhora, assim torna as recidivas recorrentes, ligadas a má utilização ou descontinuidade terapêutica. Este evento de grande impacto para saúde, contribui para seleção de microrganismo mais resistente, tornando o tratamento ou inefetivo (MUHAJ *et al.*, 2022).

Em áreas da medicina, a incorporação de novos conhecimentos à prática clínica se dá de maneira dinâmica. Para que tais avanços aconteçam, a existência de centros de pesquisas básica e aplicada é uma condição necessária, e, estudos com novos medicamentos, são de fundamental importância. Assim sendo, materiais nanoestruturados vêm sendo aplicados em diversas áreas, tais como: saúde, agricultura, cosmética, meio ambiente, entre outras (C *et al.*, 2020; CHEN, LONG; LI; CHEN, 2019), devido seu tamanho reduzido, alta superfície de contato e baixa toxicidade.

Com especificidade para área farmacêutica, estes são utilizados para resolução de problemas de diversas classes terapêuticas, como: antitumoral, antimicrobiana, anti-inflamatória, entre outras, pois, em geral, apresentam menor toxicidade, maior solubilidade e biodisponibilidade tecidual (CHARELLI *et al.*, 2022; EL-SONBATY; KANDIL; HAROUN, 2022). A área de controle de doenças infecciosas é destaque nos estudos de nanotecnologia. As nanoestruturas preparadas com metais, exibem potencial antimicrobiano de amplo espectro, com ações direcionadas às bactérias e fungos (HUQ *et al.*, 2022; OWAID *et al.*, 2022).

Diversos ensaios biológicos vêm sendo desenvolvidos frente utilizando sistemas nanoestruturados. Nestes sistemas, a resposta celular é guiada por mudanças na hidrofilia, morfologia, porosidade, cristalinidade e composição química da superfície do nanocomposto (VIET *et al.*, 2018). Assim, a bioatividade como por exemplo a capacidade antibacteriana e antifúngica, biocompatibilidade (umidade, rugosidade, porosidade, etc.), e as propriedades mecânicas são revistas permanentemente por diferentes estudos, garantindo maior eficácia dos materiais (PARVATHY *et al.*, 2022).

O óxido de grafeno (GO), material bidimensional à base de carbono, o torna elemento de ampla aplicação tecnológica e precursor para síntese de novos materiais, dada à área superficial específica, a estabilidade química, a condutividade termo-

elétrica e resistência mecânica (AĞBULUT *et al.*, 2022). O GO pode ser produzido via sonicação, agitação e expansão térmica, do óxido de grafite (FADIL *et al.*, 2022). Segundo Hummers e Offeman, os recursos materiais, correspondentes às etapas iniciais de síntese de grafeno, incluem a oxidação do grafite por mistura de ácido sulfúrico, nitrato de sódio e permanganato de potássio (HUMMERS; OFFEMAN, 1958).

Quando o GO é quimicamente modificado - óxido de grafeno reduzido rGO - surgem novas propriedades químicas e biológicas, especialmente, o aumento de solubilidade e reatividade antimicrobiana (SENGUPTA *et al.*, 2019). Tratamentos com hidrazina, hidretos, hidroquinona permitem novas estratégias de síntese desse óxido de grafeno reduzido. Esse processo químico rompe a ligação sp2 da rede e introduz grupos hidroxila ou epóxido no plano basal, enquanto que os grupos carbonila e carboxila, em conjunto com lactona, fenol e quinona são anexados às bordas (LAVIN-LOPEZ *et al.*, 2017). Os grupos funcionais deixam o rGO fortemente hidrofílico, permitindo a sua dispersão em água pura, solventes orgânicos e misturas aquosas.

Estudos anteriores, sugerem que o potencial de ação dos materiais à base de grafeno contra microrganismos, é observado após contato direto entre as bordas afiadas das folhas de rGO com as células, resultando em vazamento de material intracelular e afetando negativamente o metabolismo (QUINTEROS *et al.*, 2016). Corroborando com esta afirmativa, Perreault e colaboradores (PERREAULT *et al.*, 2015) identificaram que a ampliação da área da folha de grafeno está proporcionalmente relacionada com o aumento da taxa de inativação microbiana.

Vários estudos de análise da ação do rGO, associados com metais, sobre microrganismos patogênicos de relevância clínica foram conduzidos por vários pesquisadores, evidenciando o seu potencial antimicrobiano contra: *Escherichia coli* (KESHVARDOOSTCHOKAMI *et al.*, 2020), *Staphylococcus aureus* (CAIRES *et al.*, 2020) *Staphylococcus epidermidis* (JAWORSKI *et al.*, 2018), *Proteus mirabilis* (FENNICHE *et al.*, 2022), *Pseudomonas aeruginosa* (ELBASUNEY *et al.*, 2021), *Listeria monocytogenes* (KURANTOWICZ *et al.*, 2015)*, Salmonella entérica* (KURANTOWICZ *et al.*, 2015), *Cryptococcus neoformans* (ELBASUNEY *et al.*, 2021), *Candida albicans* (ELBASUNEY *et al.*, 2021), *Aspergillus spp*. (ELBASUNEY *et al.*, 2021), *Fusarium oxysporum,* (CHEN, JUANNI *et al.*, 2016); *Aspergillus oryzae*, *Aspergillus niger* (ALIAMRADNI; ABOLMAALI; BORANDEH, 2019).

A prata, o cobre e o zinco são elementos reativos e que melhoram as atividades químico-biológicas dos compostos derivados do grafite. Apesar do conhecimento prévio das atividades antimicrobianas da prata, a síntese de materiais contendo esse metal em condição de nanopartículas (NPs), só foi recentemente estudada (HUQ *et al.*, 2022). Com esta formulação, foi evidenciada ação imediata sobre cadeia respiratória, destruição da membrana e parede celular, de bactérias e fungos. Além disso, seguindo com sua ligação às estruturas de DNA/RNA, a replicação celular foi interrompida, e consequentemente, estabelecida a morte microbiana (POZDNYAKOV *et al.*, 2022).

As espécies reativas de oxigênio e radicais livres, produtos decorrentes da ação das nanoestruturas de prata sobre a célula microbiana, induzem a apoptose, isto é, a morte celular programada. Assim, ficam evidentes os benefícios das nanopartículas de Ag (AgNP) como agentes antimicrobianos, seguindo mecanismos de ação multifacetados, como bloqueio do ciclo de energia, ligação enzimática e a interrupção de funções celulares(KOSA; ZAHEER, 2022). Uma vez que os Ag NPs são menores que os microrganismos, a difusão celular e, consequentemente ruptura de estruturas, é um evento esperado. Dependendo do tamanho, concentração, pH do meio e tempo de exposição das nanoestruturas de prata, poderão ocorrer respostas variadas quanto à toxicidade sobre célula microbiana (SEDKI *et al.*, 2015).

Os danos físicos provocados por compostos híbridos, por exemplo, rGO combinado com Ag, sobre a membrana celular bacteriana foram demonstrados no estudo de Zhou et al., 2020 (ZHOU *et al.*, 2020) constatando a alta capacidade de adesão à superfície das bactérias *S. aureus* e *E.coli*. No estudo de Chen et al. (CHEN, LONG; LI; CHEN, 2019), com o auxílio de recursos tecnológicos de biologia molecular, evidenciaram ação dos compostos híbridos de rGO e Ag sobre célula bacteriana, e como consequência, a inativação da síntese proteica a partir de 3 horas de contato. No estudo de Bhattacherjee et al. (BHATTACHARJEE *et al.*, 2021), o rGO/Ag foi incorporado em malhas de algodão e seda apresentou maior taxa de inibição frente a *E. coli* e *P. aeruginosa*. Esses bons resultados de sinergismo podem estar associados ao fato de que as nanopartículas de prata sozinhas apresentam dificuldades na dispersão, devido suas fortes forças de adesão, entre partículas com alta energia de superfície.

Considerando os fungos, e seus elementos de reprodução, esporos ou micélios, grande variabilidade é observada na forma e componentes externos de estrutura celular. Entretanto, há poucos estudos que identifiquem a sensibilidade ou resistência de fungos aos nancompósitos de rGO/Ag. É conhecido que combinando-se os elementos nanoestruturados, prata e óxido de grafeno reduzido, há efeito sinérgico de ação inibitória para os microrganismos (ZHOU *et al.*, 2020) induzido pela lesão física pelo rGO e geração de compostos reativos de oxigênio pela prata. Fato demonstrado no estudo de Aliamrandni et al., 2019 (ALIAMRADNI; ABOLMAALI; BORANDEH, 2019), onde os testes contra *Candida albicans* e *Candida tropicalis* seguindo o método de disco difusão, o rGO/Ag apresentou melhor ação do que os compostos separadamente testados. Em relação aos espécimes fúngicos foram observadas anormalidades morfológicas como deformações na célula do *Cryptococcus neoformans* que levaram a lise total da superfície externa, que geraram não apenas a redução da população séssil, mas também na massa de biofilme (ELBASUNEY *et al.*, 2021).

Considerando as vantagens dos nanomateriais híbridos em comparação aos antimicrobianos tradicionais, as nanopartículas de Ag apresentam baixa ou nenhuma citotoxicidade para células humanas, sendo utilizadas em diversos dispositivos médicos, além de reduzir a resposta inflamatória (PRASAD *et al.*, 2017; VASILEV *et al.*, 2010).

Assim sendo os nanomateriais híbridos, por apresentarem amplo campo de aplicação, se faz necessário a análise perfil de toxicidade, onde a maioria desses ensaios é executado em modelo *in vivo* devido as respostas fisiológicas similares aos organismos vivos. Sabendo que testes em mamíferos apresentam desvantagens quanto ao custo, demora e controvérsias em comitês éticos, os ensaios em aos modelos invertebrados tem ganhado destaque. Exemplos como *Drosophila melanogaster* (MISHRA; PANDA, 2021), *Zebra fish* (PENSADO-LÓPEZ *et al.*, 2021), *Galleria mellonella* (MOYA-ANDÉRICO *et al.*, 2021) são frequentemente usados em triagens toxicológicas. Frente a este fato, a larva de *Galleria mellonella* apresenta vantagens, uma vez que a utilização experimental é mais simplificada pelo tamanho reduzido, não há necessidade de equipamentos sofisticados e é aprovado por comitês éticos (PAZIANI *et al.*, 2019). Esse invertebrado apresenta respostas imunológicas

similares aos mamíferos, onde a hemolinfa seria comparada ao sangue, e a cutícula com a epiderme.

Diante do exposto, os nanocompósitos metálicos devem ser bem explorados sobre grupos específicos de microrganismos, uma vez que as alternativas terapêuticas disponíveis nem sempre são efetivas, dada a variação biológica dos microrganismos, mais patogênicos e resistentes aos fármacos. Ainda, as condições clínicas individuais dos hospedeiros, isto é, portador de doença crônica, imunossuprimido, ou em vigência de outras comorbidades, podem comprometer o sucesso terapêutico disponível dos produtos antifúngicos. Valoriza-se então as propriedades majoritárias das nanoestruturas híbridas, biocompatibilidade e baixa toxicidade, como propostas futuras de tratamento tópico e controle das infecções fúngicas superficiais.

2. OBJETIVOS

Testar atividade antifúngica e toxicidade dos nanocompósitos rGO/Ag, com variação na concentração de prata, frente a isolados clínicos de dermatomicoses.

2.1 Objetivos específicos:

- Avaliar as características de cristalinidade, morfologia e distribuição controlada dos nanocompósitos.
- Determinar a atividade antifúngica, por microdiluição, frente à isolados de *Candida albicans, Candida parapsilosis, Epidermophyton flocossum, Microsporum canis, Trichophyton mentagrophytes* e *Trichophyton rubrum.*;
- Determinar o alvo das nanopartículas por meio de ensaio com sorbitol;
- Determinar o tempo de morte dos fungos testados frente ao nanocompósito híbrido rGO/Ag;
- Determinar possível interferência na produção de hifas pela *Candida albicans;*
- Determinar a toxicidade, *in vivo*, dos nanocompósitos sintetizados em modelo invertebrado *Galleria mellonella*.

3. ARTIGO

Non-toxic nanocomposite based on silver nanoparticles and reduced graphene oxide against agents of dermatomycosis

Bianca Gottardo [a]; Tarcísio Perfecto [a]; Andreza Zoccal [a], Taiza Maschio-Lima [a]; Thiago H. Lemes [a]; Mario H. Paziani [b]; Marcia Kress [b]; Margarete T.G. Almeida [c]; Diogo P. Volanti1 [a].

[a.] *Institute of Biosciences, Humanities, and Exact Sciences, São Paulo State University (UNESP), 2265 Cristóvão Colombo St., 15054-000, São José do Rio Preto, Brazil*
[b.] *São José do Rio Preto Medical School (FAMERP), 5416 Brigadeiro Faria Lima Ave., 15090-000, São José do Rio Preto, Brazil*
[c.] *School of Pharmaceutical Sciences of Ribeirão Preto, University of São Paulo (USP), Café Ave., 14040-903, Ribeirão Preto, Brazil*

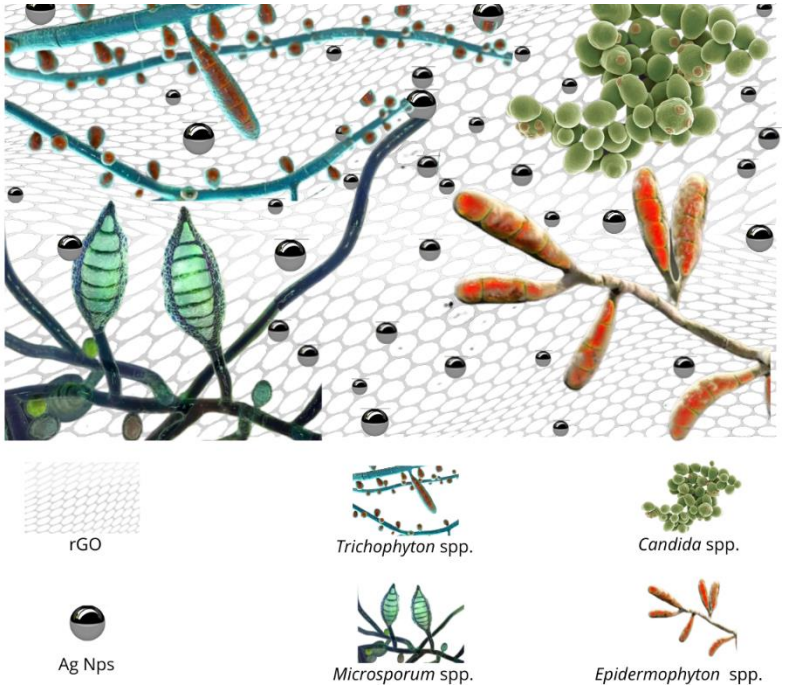

3.1 Abstract: Dermatomycoses are typical hair, skin, or nails infections caused mainly by dermatophyte and non-dermatophyte, *Trichophyton, Microsporum* and *Epidermophyton; Candida Fusarium and Scytalidium*. In addition to the esthetical impact, pain, and nail deformity, these mycoses can be a source of severe disease. The high cost for treatment, the toxicity, and the emergency for resistant pathogens justify the search for new drugs. The objective of this study was to assess the antifungal activity of reduced graphene oxide-loaded silver (rGO/Ag) nanocomposites (NCs) with different Ag concentrations (8%,10%, and 12%) against clinical isolates of dermatophytes and species *Candida*. The NCs were characterized by X-ray diffraction analysis, and the nanocomposite morphology, silver distribution on the rGO surface, and crystalline information were investigated by transmission electron microscopy. Antifungal susceptibility assay was performed by the microdilution method based on CLSI protocol, with modifications. Time kill kinetics was conducted to monitor the effect of the composite to inhibit fungal cells or promote structural changes avoiding germination. The cell toxicity was evaluated in a *Galleria mellonella in vivo* model. Minimum inhibitory concentrations (MIC) values of the rGO/Ag NCs ranged from 1.9 to 125 µg/mL. The best inhibitory activity was obtained for rGO/Ag12%, mainly against *Candida* spp. and *Epidermophyton floccosum*. In the presence of sorbitol, MIC values of rGO/Ag NCs were higher (ranging from 15.6 to 250 µg/mL), indicating the action mechanism on the cell wall. The clinical isolates of yeast and dermatophytes were inhibited at a minimum of 6h and 24h, respectively, but after 2h and 12h, they had initial antifungal interference. All hybrid formulations of rGO/Ag NCs were not toxic for *Galleria mellonella*. This study provides insights into an alternative therapeutic strategy for controlling dermatomycoses..

Key-words: Dermatomycoses, Reduced graphene oxide, Ag nanoparticles, antifungal.

3.2 Introduction

The superficial and cutaneous mycoses worldwide, with diagnosis and treatment associated with several difficulties.[1] The main etiological agents of superficial mycoses are dermatophytes: *Trichophyton, Microsporum and Epidermophyton*. According to the anatomical site of involvement, they can invade humans and animals with keratinized tissues (hair, skin or nails), causing tinea corporis, pedis, manuum, and unguium.[2] Moreover, some yeasts of *Candida albicans* and non-albicans are also present.[3,4]

Epidemiological studies from tropical regions (high temperature and humidity) show dermatomycosis as a disease of difficult treatment, especially for patients with chronic diseases, immunosuppressed or under antibiotics treatment.[5,6] Unfortunately, the diagnostic process is prolonged, and, therefore, the remedy adopted is usually empirical, contributing to therapeutic failure. Antimicrobial resistance is another problem in clinical practice, especially for azoles and polyenes drugs.[7,8]

Recently, new therapeutic alternatives have been necessary, and nanoparticles are presented as good resources for microbial control. They usually have lower toxicity, greater solubility, and tissue bioavailability, with excellent activity against tumors, microorganisms, and inflammation.[9,10] The nanoparticles (NPs) with noble metals, such as silver (Ag), gold (Au), copper (Cu), have antimicrobial potential through immediate blocking of the respiratory chain, cell components destruction, and inhibiting the replication of DNA/RNA.[11] In addition, the combination of these metals with a non-toxic matrix increases the field application. The rGO is an alternative considering its properties: two-dimensional properties, high thermal and structural defects, high surface area, and involved in cellular membrane stress.[12,13]

New strategies have emerged with a combination of Ag NPs and reduced graphene oxide (rGO) to minimize cell toxicity.[14] Interesting inhibition action has been shown against pathogen bacteria, such as *Escherichia coli* [15], *Staphylococcus aureus* [16], *Proteus mirabilis* [17], *Pseudomonas aeruginosa* [18] and *Salmonella enterica.*[19]

Besides, the use of metals with antimicrobial activity is also studied the route of administration, the cytotoxic and genotoxic effects of AgNPs are also dependent on the size, dose, and coating of the nanoparticles.

Cryptococcus neoformans, *Candida albicans*, *Aspergillus* spp. as fungal microorganisms were also faced with rGO/Ag nanoparticles [20]. The synergistic effect of these elements can reduce the spore germination or germinative tube from the fungi cell and cause morphological changes.[21]

Considering the application fields of NCs, the toxicity analysis is required. Usually the toxicity profile of these nanoparticles is frequently obtained by *in vitro* tests, but it should be executed with *in vivo* once these models have similar physiological responses of living organisms. The toxicological testing using mammals is expensive, time-consuming, and ethically debatable. For this reason, non-mammalian animal models such as *Drosophila melanogaster* [22], *Zebra fish* [23], *Galleria mellonella* [24] are often used in toxicological screenings. In comparation with the other *in vivo* models, the *G. mellonella* has a lot of advantages: easy manipulation, does not require much space or special infrastructure, low biohazard risk, and ethically accepted.

The nanomaterials of rGO based on silver were never tested against dermatophytes. Thus, this study aimed to synthesize non-toxic silver-loaded reduced graphene oxide (rGO/Ag) nanocomposites (NCs) under different Ag concentrations and check the antifungal performance against clinical isolates of dermatophytes and *Candida* spp.

3.3 Results and discussion

Currently, skin infections are a significant health care problem due to chronic and recurring public health problems [25]. *Candida* spp. and dermatophytes have emerged as the most acute infections agents and become increasingly resistant against the available antifungal drugs [26]. Therefore, nanocomposites have been used as antimicrobial products for several years, but the activity of rGO/Ag NCs against dermatophytes has not yet been evaluated.

Considering the NCs characterization, the XRD patterns of pure rGO in comparison with different contents of Ag in the rGO/Ag composite are shown in Figure 1. With the diffraction patterns, we can identify the success in obtaining the rGO since it is possible to index the broad peak chracteristic of the graphene

plane (002) in 2 theta equal to 43º.[27] This lower intensity peak is due to the reduction process of graphene oxide already presented by previous studies. [28] Furthermore, it is possible to identify the diffraction planes of the cubic structure of the metallic Ag, with the lattice planes (111), (200), and (202) indexed, corresponding to the COD standard 9012961. No secondary phases or contaminants were found in the samples with these analyses.

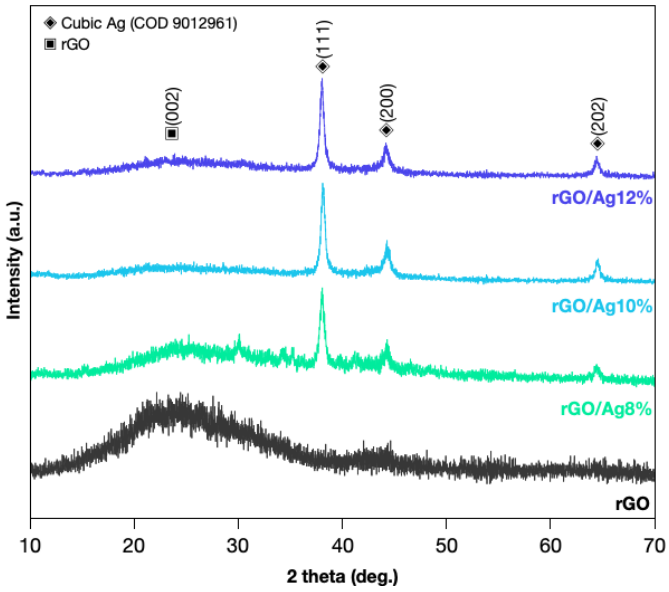

Figure 1: XRD patterns of the rGO, Ag, and rGO/Ag NCs prepared with different Ag content.

Scanning transmission electron microscopy (STEM) was performed to understand how the Ag is distributed in the rGO and shown in Figure 2 a-b. The nanosheet morphology can be seen in the image (Figure 2a) attributed to the rGO structure. In Figure 2b, it is possible to identify a second structure with a different charge density associated with metals. A STEM image of the mixture of rGO/Ag NCs indicates the formation of a few numbers of AgNPs on the surface of rGO nanosheets. This structure was associated with the nanoparticles of Ag, with a variable size of 5-30 nm. Sedki [29] presented Ag NPs with similar dimensions forming in a spherical shape ranging from 11 to 20 nm. In Figure 2c, the high-resolution transmission electron microscopy (HRTEM) of a single particle of Ag, we can see the lattice fringes of cubic ordered Ag (0.23 nm, (111)).

Finally, with the selected area electron diffraction (SAED) technique performed in the same microscope, the diffraction pattern from cubic Ag was

indexed. Almost all most intense diffraction planes from Ag were indexed. Since the rGO structure has an amorphized feature, neither lattice fringes nor diffraction patterns were observed in the SAED.

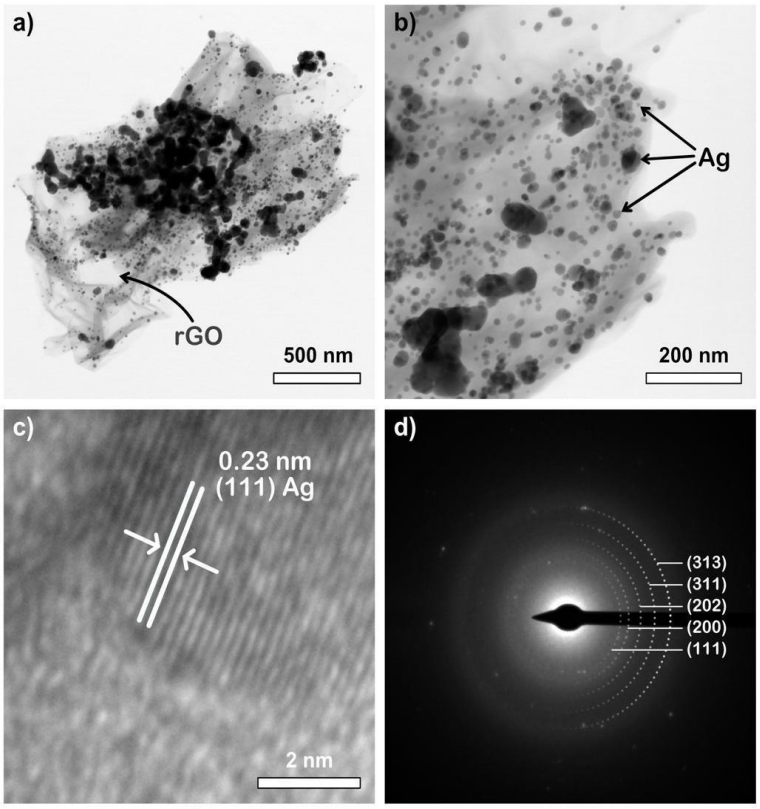

Figure 2: TEM images (a and b) with different magnifications of rGO/Ag12% sample scales. The image c) depicts the HRTEM, and the d) the SAED from the rGO/Ag12% samples were observed.

Exciting results of fungal inhibition in this present study because all dermatophytes, never tested before in previous studies (Table 1), and *Candida* spp. were sensitive to rGO/Ag NCs. Regarding the initial antifungal susceptibility test with rGO against dermatophytes, the ranged MIC values were 125-250 µg/ml, and for yeasts, there was no inhibition (Figure 3, columns 2-3). It is important to consider that dermatophytes have the largest cell size and high structural variability that could increase the contact surface area with rGO. Similar results were described by Sawangphyruk [33] against *Fusarium oxysporum*, *Aspergillus niger*, and *Aspergillus oryzae*. Moreover, the antifungal response of Ag NPs was detected for all microorganisms (MIC 250µg/mL), except for EF1-2 e MC1-2 because of their resistance. Corroborating results were described by Prasad [17] once rGO presented

advantaged antimicrobial activity in comparison to Ag NPs, although for bacteria. The potential action of graphene-based nanomaterials is associated with physical cell damage. The direct contact between the sharp edges of the rGO sheets with fungal cell can physically damage the external structure, resulting in intracellular material leakage and negatively affecting metabolism.[34] The research performed by Perreault [35] corroborates with this data and explains that the expansion of the graphene sheet area is proportionally associated with the increase of microbial inactivation percentage.

Table 1: Antimicrobial susceptibility analysis of all NCs shown in this work against dermatophytes agents and *Candida* spp, and antimicrobial performance of rGO/Ag in previous studies.

References	Tested Microorganisms	Summary inhibition results
This work	*E. floccosum, M. canis, T. mentagrophytes, T. rubrum, Candida albicans, Candida parapsilosis*	*E. floccosum* 3.9µg/mL; *M. canis* 15.6µg/mL: *T. mentagrophytes* 3.8µg/mL; *T rubrum* 62.5µg/mL; *C. albicans* 1.9µg/mL and *C. parapsilosis* 3.9µg/mL
[20]	*Cryptococcus sp., C. albicans, Aspergillus sp.,*	*Cryptococcus* 62.5µg/mL; C. *albicans* 125µg/mL; *Aspergillus*: 15.67µg/mL
[21]	Zygomycetes	Agar with NCs, reducing the colony diameter
[30]	*E. coli*	Inhibition activity at 100µg/mL
[31]	*E. coli* and *S. aureus*	*E. coli* 32 µg/mL *S. aureus* >250 µg/mL
[32]	*E. coli, S. aureus, P. aeruginosa, C. albicans*	Inhibition activity only against bacteria

Several profiles of antifungal activity were noted, EF1-2 and MC1-2 presenting resistance to Ag NPs, and for TM1-2, TR1-2, CA1, CP1, a minimum action was observed, with MIC value of 250 µg/mL (Table 2). Analogous results of variable activity were also described before by Gottardo [36] against *Candida* spp. Usually, this source allows originated microorganisms with higher resistance and virulence, considering the pressure exerted by the external environment.[37] *Trichophyton* spp was previously studied by Kim [38], especially *T. mentagrophytes*, and for the same product, presented a better MIC value than ours, 1-4 µg/mL. It is essential to consider the origin of samples of both studies once they evaluate ATCC strains and clinical isolates.

The hybrid nanocomposites (rGO/Ag NCs) showed higher antifungal activity when compared with isolated nanoparticles (synergistic effect). It is important to consider this effect for all yeast; once it was resistant to rGO and with a hybrid formulation, the antifungal activity was relevant. The rGO/Ag8% (Figure 3 at columns 6-7) presented MIC of 3.9 µg/mL for yeasts and 15-62,5 µg/mL for dermatophytes. The rGO/Ag10% (Figure 3 at columns 8-9) MIC was 1.9 µg/mL for CA1 and 7.8 µg/mL for CP1; for dermatophytes, 7.8-125 µg/mL with the best activity for EF1, 7.8 µg/mL. Considering rGO/Ag12% (Figure 3 at columns 10-11), the best antifungal activity was seen against yeasts, 1.9 µg/mL MIC, and for dermatophytes, ranged MIC from 3.9-62,5 µg/mL for EF1, TM1, MC2 e TR1, respectively.

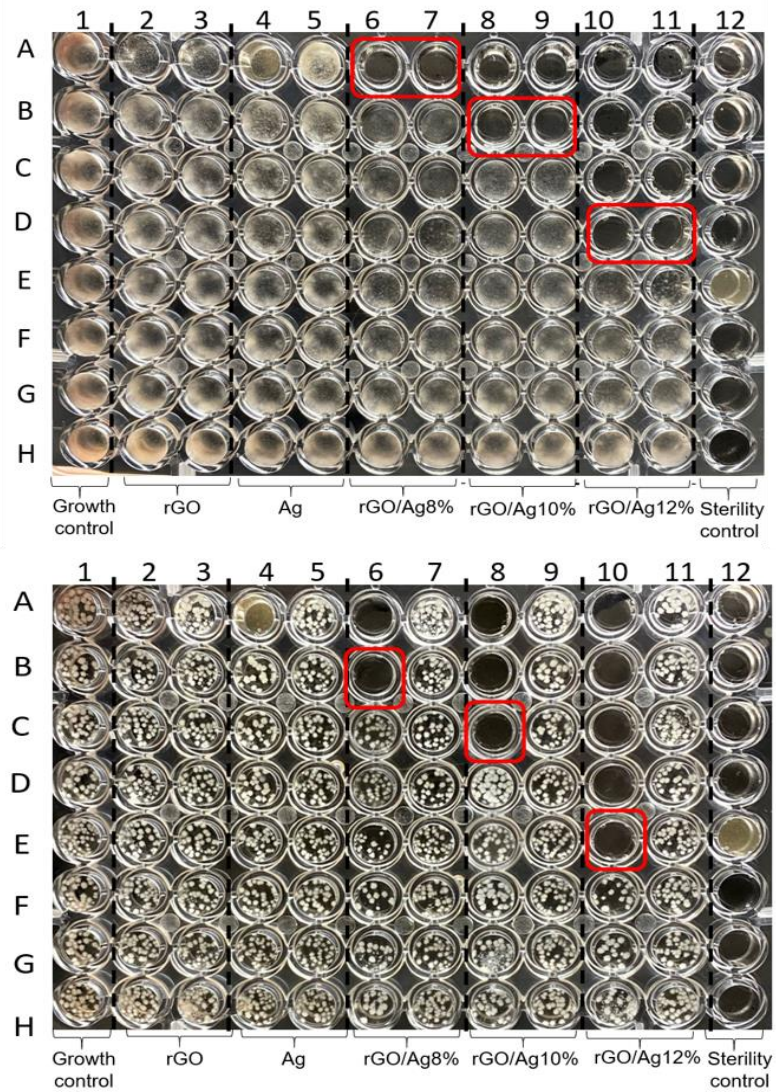

Figure 3: Antifungal susceptibility test of rGO, Ag NPs, rGO/Ag NCs, and controls against EF1 and CA1 (up and down, respectively), showing the best antifungal activity.

These results corroborate Elbasuney [20], considering the antimicrobial activity against the fungal cell; nevertheless, for different species: *Aspergillus* sp., ranged MIC from 0.97–15.62 µg/mL, and 15.62–125 µg/mL for *Candida* sp. and *Cryptococcus* sp. Our study shows excellent results of inhibition for all *Candida* species - MIC value 1.9µg/mL when compared with the date from Elbasuney.[20] This fungal genus is important in superficial, subcutaneous, and deep infections, sometimes presenting antifungal resistance patterns for any class of drugs, azoles, polyenes, and echinocandins.[39]. Another study presented a higher MIC at >250 but tested against *Staphylococcus aureus.*[31]

Although the cellular inhibition targets may differ between fluconazole and NCs, the rGO/Ag12% showed the best MIC results, except for TR1-2. This activity should be considered for future studies once the presence of fluconazole-resistant isolates would have a new therapeutic alternative for their control. The susceptibility differences found for different species of fungi in this study occurred as expected since physiological responses diverge between them. In this sense, the stage of cell reproduction and the expression of genes for new proteins may cause changes in sensitivity.[40]

Karthik [41] and Pusty [21] confirmed the synergic effect of Ag and rGO, similar results from our study, although evaluated bacteria and zygomycetes, respectively.The antimicrobial activity of hybrid nanoparticles is present due to the physical interaction with rGO sharp edges that disrupt the cell structures, independent of microorganisms, facilitating the delivery of silver particles.[16,42]

Table 2: Antifungal susceptibility analysis of Rgo, Ag NPs, RGO/Ag NCs, and fluconazole against samples of dermatophytes and *Candida* spp.

Isolates	MIC NCs (μg/mL)					
	rGO	Ag	rGO/Ag8%	rGO/Ag10%	rGO/Ag12%	Fluconazole
CA1	-	250	3.9	1.9	1.9	3.9
CP1	-	250	3.9	7.8	1.9	7.8
EF1	250	-	15.6	7.8	3.9	15.6
EF2	250	-	31.2	31.2	15.6	31.2
MC1	250	-	62.5	125	31,2	31.2
MC2	250	-	62.5	62.5	15.6	15.6
TM1	250	250	31.2	62.5	7.8	15.6
TM2	250	250	62.5	125	31.2	62.5
TR1	125	250	62.5	31.2	62.5	4
TR2	125	250	62.5	62.5	125	8

Moreover, this synergistic effect between reduced graphene oxide and silver is explained through the physical damage and ROS (Reactive Oxygen Species) production (Figure 4). In the Chen [30] using molecular analysis presented that rGO/Ag kills bacteria disrupting the cell membrane and releasing the Ag+ inside the cytoplasm to further interrupt protein functions. This event could explain the improved activity in hybrid nanocomposite once the Ag NPs present difficulties in dispersion due to their strong adhesion forces between particles with high surface energy, and, the reduced graphene oxide can fix metallic nanoparticles at hyphae interfaces as surfactant agents. [43,44] In addition, sorbitol is an osmo-stabilizer protecting the cell wall from lysis caused by antifungal products. [45] The supplemented RPMI medium with sorbitol shows the interface to determine compounds that directly interfere in cell wall synthesis and control cell wall mechanisms. This event was studied for us, considering one yeast and one mould, CA1 and EF1, respectively. Our findings indicated the cell wall is the target structure for our hybrid NCs, once the MIC values become higher (Figure S2). The potential of inhibitory action of rGO/Ag NCs was modified, presenting increased MIC value in the presence of sorbitol (Table 3).

These findings present a specificity of rGO/Ag NCs for cell wall on fungi isolates, emphasizing the non-existence of previous tests against dermatophytes agents, only for bacteria, phytopathogenic fungi, and *Candida* ATCC strains.[46,47]

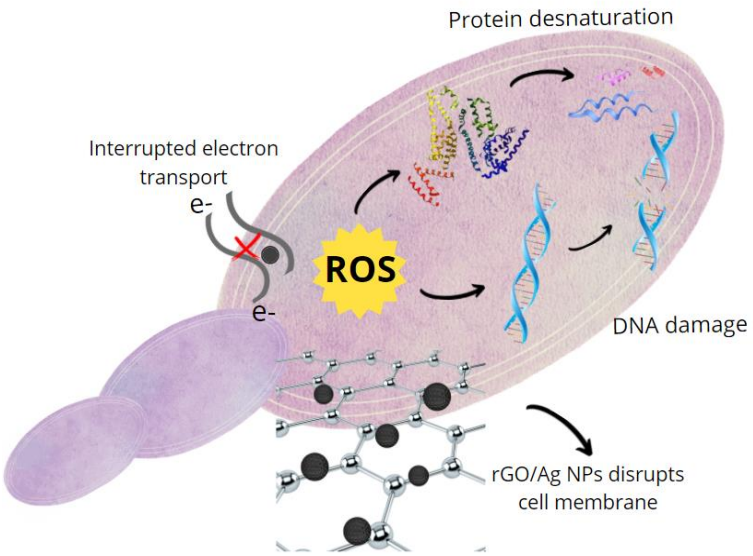

Figure 4. Demonstrative image of NCs activity against *Candida* spp. Source: The autor.

The success of the treatment of fungal disease is time-dependent on drug activity, especially for immunocompromised patients. Therefore, studying the time-kill is essential to investigate the better treatment strategies for fungal diseases. The antifungal effects of rGO/Ag were conducted using the colony counting method with a fixed amount (MIC value) incubated with fungi inoculum. Except for *T. rubrum*, where rGO/Ag10% MIC was lower, the best results occurred for all rGO/Ag12% samples. It was observed that yeasts inhibition starts after two hours of contact with rGO/Ag NCs, and dermatophytes, 12 hours. For Zhou [31], the rGO/Ag did not have a practical activity of less than 2 hours, but against *Escherichia coli*.

Table 3: Comparative analysis of MIC values of non-supplemented and supplemented medium with sorbitol.

FUNGI	- SORBITOL /NCs MIC (µL/mL)			+ SORBITOL /NCs MIC (µL/mL)		
	rGO/Ag8%	rGO/Ag10%	rGO/Ag12%	rGO/Ag8%	rGO/Ag10%	rGO/Ag12%
E.floccosum	15.6	7.8	3.9	250	125	31.2
C.albicans	3.9	1.9	1.9	125	62.5	15.6

Nevertheless, the time-kill for both occurred after 6 and 24 hours, respectively (Figure S4). These differences in inhibition times could be explained because the isolates have different origins and individual biological aspects.[48] The loss of cell viability increased gradually with a rise incubation time. Similar to our results, Sedki [29] presented a short period of cell reduction with more than 4 hours, Gu [49] showed the inhibition with 7 hours, and Chen [30] with 3 hours, but both against bacteria.

Every individual culture obtained from the time-kill assay after plating on Agar Sabouraud demonstrated the diameter reduction of the colony in 80% (Figure 5), followed the formula of colony reduction percentage. This analysis proves that the rGO/Ag NCs interfere with the growth of all dermatophytosis agents. Individual characteristics of the colony for each species must be considered and permanently were reduced after comparison between treated and non-treated groups. This event was previously reported considering 100 µL/m of rGO, in contact with *Aspergillus* spp. with an expressive colony reduction.[33]

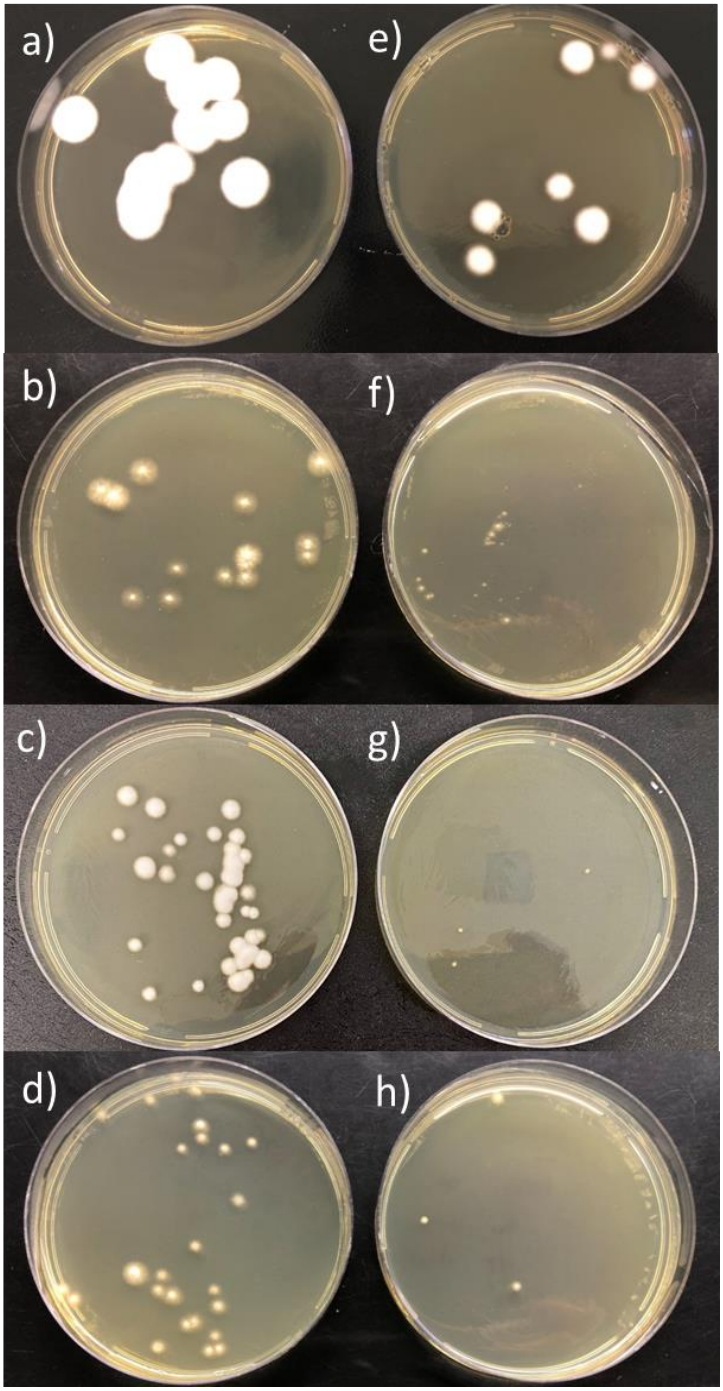

Figure 5: Image of *Trichophyton mentagrophytes*, *Epidermophyton floccosum, Trichophyton rubrum*, and *Microsporum canis* colonies showing the inhibition and diameters reduction on Petri dishes: on the left, a, b, c, and d - control group without rGO/Ag12% NCs, and on the right, e, f, g, and h - treated group with rGO/Ag12%.

The rGO/Ag interference test on *Candida albicans* cells was performed by optical microscopy to see the hyphal inhibition with and without hybrids NCs. The control culture showed a range of 69 cells/field - 400x magnitude with hyphae; 16 at MIC/2 concentration and 28 at MIC/4 concentration, representing 59.5 to 76% of cell reduction (Figure 6). The absence of hyphae proves that the

rGO/Ag NCs inactivate the germination of *C. albicans*, cell swelling, and lysis as theprevious description.[50] Data different from ours, described by Kichukova [51], did not detect action by rGO/Ag against *C. albicans*.

The rGO/Ag causes oxidative stress through the imbalance between the production of reactive oxygen species and the cellular capacity of detoxification of the reactive intermediates.[51] This fact can explain the short time to kill all clinical samples, reduced size of dermatophytes colony, and interrelation in cell germination of *Candida* in this present study. Thus, it is supposed that the hybrid rGO/Ag NCs can modify microbial morphology, changing membrane permeability by physical damage affecting fungi cellular responses.

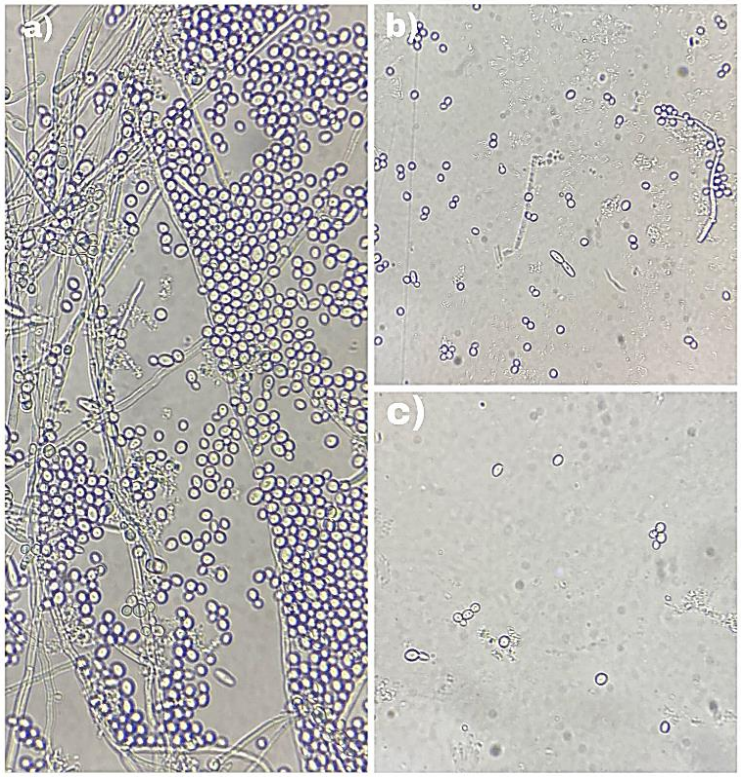

Figure 6: Images from optical microscopy (magnitude of 400x) showing the Anti-hyphal activity after 3 h of contact of rGO/Ag12%NCs - MIC/2 (c) and MIC/4 (b), in comparison with control (a). It is possible to see the reduction of *Candida* hyphae and a lower number of cells with rGO/Ag NCs.

For the practical application of antifungals, toxicological tests are requested to minimize patient harm, particularly for that formulation with Ag. The oral route is often used for fluconazole, so the prolonged time causes hepatotoxic damage.[52] These preliminary toxicity tests in vivo model of *Galleria mellonella* could be composed as a therapeutic alternative.

The *in vivo* toxicity assays in *Galleria mellonella* have an advantage when compared with traditional mammalian models: simply and economically obtained on a large scale (life cycle in 7–8 weeks); preserve without special laboratory equipment, reduced size inoculation, and ethically accepted.[53] The hybrid NCs were performed by injection and bathed in *Galleria mellonella* larvae. Both methods have importance because of the insect cuticle works as a barrier between mammalian skin and the hemolymph with mammalian blood. The insect hematocytes act as phagocytes and show some proteins with high similarity to antibodies from humans.[54]

Figure S5 shows the graphic with obtained results. Neither pure rGO nor rGO with Ag concentrations showed a toxic profile, keeping more than 80% of the larvae alive during the trial period (until 7 days). The toxicity profile is only represented by the capacity of tested material to kill at least 50% of the *G. mellonella* population. For Bhattacharjee [32], the rGO/Ag NCs showed toxicity, reducing more than 30% of cellular viability.

This finding is relevant once most Ag NPs produce numerous toxic effects due to the generation of ROS, causing DNA damage and apoptotic cell death. Whereas the pure quaternary ammonium tested as a toxic compound was able to kill all the larvae 24 h after the injection, both inoculated and bathed. Face to face with pure rGO, this model presents some sensibility, but it can't be considered as a toxic compound. The negative toxicity control (PBS), as expected, was not able to kill any larvae, presenting a non-toxic profile.

All synthesized products were shown to be non-toxic with statistical significance ($P < 0.05$) and the not associated rGO. $P < 0.05$, which means that has a probability of only 5% that results of in vivo toxicity could not be accurate. A lower P-value shows a little probability of this event occurring. The absence of toxicity might be explained because phagocytosis by macrophages declined after being treated with nanoparticles with sizes less than 260 nm, and the inflammation response was not observed to be a significant intensity.[55] These findings reinforce the excellent performance of rGO with or without silver concentrations.

Conclusions

This study shows a synthesis of hybrid nanocomposites containing a non-toxic matrix represented by reduced graphene oxide, and by a fungicidal agent, nanoparticularized silver (Ag NPs). Therefore, the nanocomposites present spherical nanostructured silver between 5-30nm in reduced graphene oxide, demonstrated by electron microscopy and XRD analysis.The rGO/Ag hybrid was tested against 10 clinical isolates of dermatomycoses showing synergistic antifungal activity against dermatophytes and *Candida* spp (MIC of 125-1.9µg/mL), with sensitivity for *E. floccosum* and *Candida albicans* isolates: MIC 3.9 and 1.9 µg/mL. Interestingly, the remarkable antifungal performance shown by NCs can be attributed to the strength of interaction of rGO/Ag with the surface of the fungal cell wall, with specificity for some receptors, demonstrated by the microdilution test with 0.8M sorbitol supplementation. In addition, the fungal structures showed interference from 2 hours and 12 hours for yeasts and dermatophytes, respectively. Yeasts had inhibition of hyphae formation, and dermatophytes size reducedution of the colony diameter. The non-toxic profile *in vivo* could be explain due to the homogeneous dispersion of Ag NPs in the rGO matrix, which protect the host against cellular damage, presented by *Galleria mellonella* assay.The study is unprecedented, since the antifungal action of rGO/Ag on dermatophytes has never been evaluated before.The findings contribute to new therapeutic perspectives for the control of superficial fungal diseases, especially due to the broad activity spectrum of nanoparticulate materials, such as biocompatibility and low toxicity.

Supporting Information

Antifungal susceptibility test mapping against dermatophytes and yeasts;

MIC tests supplemented with sorbitol against Epidermophyton floccosum and Candida albicans;

Time kill test with control plates and treated with rGO/Ag NCs, showing the total inhibition

Graphic image of toxicity assay of rGO/Ag NCs in vivo model of Galleria mellonella.

3.5 Experimental section

2.5.1 Materials

Graphene oxide, sodium dodecyl sulphate ($NaC_{12}H_{25}SO_4$), silver nitrate ($AgNO_3$, 99% purity), ethanol (CH_3CH_2OH, ≥98% purity), sodium hydroxide (NaOH, ≥98% purity), sodium dihydrogen phosphate dihydrate ($NaH_2PO_4 \cdot 2H_2O$, ≥99.0% purity), sodium borohydride ($NaBH_4$), Sorbitol ($C_6H_{14}O_6$), Fluconazole (Sigma-Aldrich®) Sabouraud Broth and Agar (SB/AS Oxoid®), Phosphate-buffered saline (PBS), and Roswell Park Memorial Institute- RPMI (1640 medium /Sigma-Aldrich®), dimethyl sulfoxide - DMSO (C_2H_6OS, 99.9% purity/ Synth®), quaternary ammonium compound (QAC), sodium hypochlorite. Finally, aqueous solutions were prepared with Milli-Q ultrapure water with a resistivity of 18.2 MΩ·cm (at 25 °C).

2.5.2 Synthesis of rGO and rGO/Ag NCs

The Ag/rGO NCs were prepared with different Ag concentrations, i.e., rGO/Ag8%, rGO/Ag10%, and rGO/Ag12%. Initially, 33.9 mg of GO and 13.56 mg of sodium dodecyl sulphate (mass ratio 10:4 GO/SDS) were dispersed in 20 mL of ethanol. The suspension was placed in an ultrasonic bath for 20 minutes. Then, an excess of 620 mg of $NaBH_4$ was added, and the suspension was kept in the ultrasonic bath for another 20 minutes. The solutions containing 8%(2.71mg), 10%(3.4mg), and 12%(4.32mg) of silver in relation to the mass of GO were prepared with 10 ml of ethanol under magnetic stirring. After complete reaction, the precipitate was washed with deionized water and ethanol centrifuged for 10 minutes, at 7500 RPM, until the solution became colorless. The composite was oven-dried at 95 °C and manual deagglomerated (Figure 7).

Figure 7: Illustrative scheme of NCs synthesis. Source: The autor.

3.5.3 Characterization of NCs

The rGO and rGO/Ag NCs were analysed by X-ray diffraction (XRD) with Rigaku equipment, model MiniFlex 300 (Cu Kα radiation, λ = 1.5418 Å), with a 2θ from 10° to 70° at 2° min−1. The Scherrer equation valued the crystallite dimensions of the examples to the full width at half-maximum (fwhm) of the (202), (200), and (111) peaks. For morphology and size of rGO/Ag NCs the transmission electron microscopy (TEM, FEI TECNAI G2F20) was operated at an accelerating voltage of 200 kV. The high-resolution transmission electron microscopy (HRTEM) images of Ag planes were taken by a JEM-2100 model instrument (JEOL, Tokyo, Japan) operated at an accelerating voltage of 200 kV. The selected area electron diffraction (SAED) technique was performed in the same microscope to analyze the diffraction pattern from cubic Ag. Moreover, to verify the Ag distribution in the rGO, scanning transmission electron microscopy (STEM) was used.

3.5.4 Antifungal Susceptibility and Sorbitol analysis

Tests of antifungal activity were conducted with dermatophytes and yeasts from human isolates (10 specimens) from nail, skin, and scalp; all belonged to the collection culture of the Faculty of Medicine of São José do Rio Preto (FAMERP): *Epidermophyton floccosum* (EF1 and EF2), *Microsporum canis* (MC1 and MC2), *Trichophyton mentagrophytes* (TM1 and TM2), *Trichophyton rubrum* (TR1 and TR2), *Candida albicans* (CA1), and *Candida parapsilosis* (CP1). The rGO/Ag NCs, rGO, Ag NPs, and fluconazole® were evaluated in triplicate (100 µL of RPMI with inoculum and 100 µL of each NCs), following Clinical & Laboratory Standards Institute protocol: CLSI M38-A2 [53] for dermatophytes, and M27-A3 [54] for *Candida* spp, with modifications for hybrid nanocomposite.

Microplates (TPP®, Switzerland) were prepared after growing dermatophytes and yeasts, and the inocula were adjusted to 1.5x103 cells. Two columns received NCs, dissolved in DMSO (Synth®, Diadema, Brazil), at 10%, at ranges of 250-1.9µL/mL, and 250-0.007µL/mL, for dermatophytes and yeast, respectively (Figure S1). All cultures were incubated at 30 °C, for 24h, for *Candida*, and for seven days, for the dermatophytes.

To investigate the action's target of NCs, the sorbitol 0,8 M in RPMI medium was performed, following microdilution protocol for dermatophytes and *Candida* spp., and adopting a method described by Castro & Lima.[42]

3.5.5 Time kill assay

The action analysis of NCs on fungi cell viability versus contact time occurred according to the protocol of Klepser [58], with some modifications. Initial inoculum of the culture of fungi (50µl) was transferred to Falcon tube with 4.95 ml of SB, and after, 500 µl was introduced to another tube with 9.5 ml of SB. After this, 1ml was removed and introduced rGO/Ag NCs (1 mL of 2x MIC values) demonstrated in the Figure S3. Each 2 and 12h, 20 µL of yeast and dermatophytes culture were streaked on Sabouraud Agar Dextrose Medium (OXOID, Basingstoke, United Kingdom) and incubated at 30°C. After 1-5 days, the inhibitions were determined by visual reading measuring the colony diameter and counting-cell growing/inhibition with and without rGO/Ag12% NCs. The antifungal effect was expressed in the percentage date of mycelial growth inhibition and calculated by the formula: dC-dT/dC x 100% described by Sawangphruk.[33] DC is the average diameter (mm) of the fungal colony as control and dT of the fungal colony as a treated group with NCs.

3.5.6 Hyphal inhibition test

The culture of *Candida albicans* and rGO/Ag NCs were prepared into a plate of 96 wells to evaluate the hyphal inhibition, as the protocol described by Bernardes.[59] Sabouraud Broth with 10% of animal serum (SB10%serum) was inoculated with 10µL and 20µL of rGO/Ag NCs, to obtain the final concentration of MIC/4 and MIC/2, respectively.

The fungi inoculum was prepared considering turbidity of 0.5 Mac Farland standard tube by spectrophotometer reading, and 100µL added into SB10%serum (1.9mL), following incubation at 37ºC for 3 hours. The results were considered after counting fungal cells in Neubauer Camera and hyphal structure evaluated by light microscope magnification power (400X).

3.5.7 *In vivo* toxicity test

The toxicity of rGO and rGO/Ag NCs was determined in a *Galleria mellonella* in vivo model. [60] Groups of 10 *G. mellonella* larvae (weighing between 250−300 mg each) were randomly selected. The toxicity of the hybrid NCs and rGO were tested by artificial inoculation and bath. For the injection step, 5 µL (concentration of 250µg/ml) of each compound was introduced into the larvae's last right proleg using a Hamilton microsyringe for gas chromatography model 7000.5 KH. Between injections, the microsyringe was rigorously washed 3 times with sodium hypochlorite, 70% ethanol, and autoclaved water. For bath assay, the larvae were submerged in the suspension of each composition for 2 seconds and dried at laboratory temperature. PBS and QAC were used as a negative and positive control of toxicity, respectively. The toxicity profile is considered when the tested product eliminates at least 50% of the larvae group. The larvae were incubated at 28°C, deprived of feed and direct lighting, and removed from the prepupae to delay their metamorphosis every 24 hours. The statistical analyses were performed by the Log-rank method (Mantel-Cox) using the GraphPad Prism 5 software. All tested formulations followed the protocol by Gottardo. [36]

3.6 Acknowledgments

The authors are thankful for the financial support of the São Paulo Research Foundation, FAPESP (Grants FAPESP 2018/00033-0) National Council for the Improvement of Higher Education (CAPES), SISNANO/ MCTI, FINEP, and Embrapa AgroNano research network. The FE-SEM facilities were provided by the Nanotechnology National Laboratory for Agriculture (LNNA), Embrapa Instrumentation, São Carlos, São Paulo, Brazil. TEM facilities were provided by LCE/DEMa/UFSCar. We acknowledge the Multi-User Laboratory (LMU) at São Jose do Rio Preto (FAMERP).

3.7 References

1 A. K. Gupta and M. Venkataraman, *J. Dermatolog. Treat.*, 2021, **0**, 1–8.

2 P. M. Ridzuan, C. M. Nazira, M. Ruth, C. N. Abdul Rassip, M. H. Nur Raihan, S. Ismail, N. I. A. Rahman, E. A. Suzima and H. Azhan, *J. Sci. Math. Lett.*, 2019, **8**, 6–15.

3 G. Ginter-hanselmayer and P. Nenoff, *Clinically Relevant Mycoses*, Springer International Publishing, Cham, 2019.

4 V. G. Mello, H. Escudeiro, A. C. V. B. Weckwerth, M. I. Andrade, A. E. Fusaro, E. B. de Moraes, L. da S. Ruiz and I. M. F. D. Baptista, *Mycopathologia*, 2021, **186**, 71–80.

5 A. Casadevall, *Annu. Rev. Immunol.*, 2022, **40**, 121–141.

6 L. Davidson, M. G. Netea and B. J. Kullberg, *J. Fungi*, 2018, **4**, 9.

7 A. Khurana, K. Sardana and A. Chowdhary, *Fungal Genet. Biol.*, 2019, **132**, 103255.

8 S. Gnat, D. Łagowski and A. Nowakiewicz, *J. Appl. Microbiol.*, 2020, **129**, 212–232.

9 S. Fernando, T. Gunasekara and J. Holton, *Sri Lankan J. Infect. Dis.*, 2018, **8**, 2.

10 R. Lakshminarayanan, E. Ye, D. J. Young, Z. Li and X. J. Loh, *Adv. Healthc. Mater.*, 2018, **7**, 1–13.

11 S. Prabhu and E. K. Poulose, *Int. Nano Lett.*, 2012, **2**, 32.

12 A. Lerf, H. He, M. Forster and J. Klinowski, *J. Phys. Chem. B*, 1998, **102**, 4477–4482.

13 C. A. Zito, T. M. Perfecto and D. P. Volanti, *Sensors Actuators, B Chem.*, 2017, **244**, 466–474.

14 S. Barua, S. Thakur, L. Aidew, A. K. Buragohain, P. Chattopadhyay and N. Karak, *RSC Adv.*, 2014, **4**, 9777.

15 T. G. Volova, A. A. Shumilova, I. P. Shidlovskiy, E. D. Nikolaeva, A. G. Sukovatiy, A. D. Vasiliev and E. I. Shishatskaya, *Polym. Test.*, 2018, **65**, 54–68.

16 T. Tian, X. Shi, L. Cheng, Y. Luo, Z. Dong, H. Gong, L. Xu, Z. Zhong, R. Peng and Z. Liu, *ACS Appl. Mater. Interfaces*, 2014, **6**, 8542–8548.

17 K. Prasad, G. S. Lekshmi, K. Ostrikov, V. Lussini, J. Blinco, M. Mohandas, K. Vasilev, S. Bottle, K. Bazaka and K. Ostrikov, *Sci. Rep.*, 2017, **7**, 1591.

18 M. A. Quinteros, V. Cano Aristizábal, P. R. Dalmasso, M. G. Paraje and P. L. Páez, *Toxicol. Vitr.*, 2016, **36**, 216–223.

19 M. Saravanan, S. K. Barik, D. MubarakAli, P. Prakash and A. Pugazhendhi, *Microb. Pathog.*, 2018, **116**, 221–226.

20 S. Elbasuney, G. S. El-Sayyad, H. Tantawy and A. H. Hashem, *RSC Adv.*, 2021, **11**, 25961–25975.

21 M. Pusty, A. K. Rana, Y. Kumar, V. Sathe, S. Sen and P. Shirage, *ChemistrySelect*, 2016, **1**, 4235–4245.

22 M. Mishra and M. Panda, *Free Radic. Res.*, 2021, **55**, 919–935.

23 A. Pensado-López, J. Fernández-Rey, P. Reimunde, J. Crecente-Campo, L. Sánchez and F. Torres Andón, *Nanomaterials*, 2021, **11**, 1784.

24 L. Moya-Andérico, M. Vukomanovic, M. del M. Cendra, M. Segura-Feliu, V. Gil, J. A. del Río and E. Torrents, *Chemosphere*, 2021, **266**, 129235.

25 N. M. Martinez-Rossi, N. T. A. Peres, T. A. Bitencourt, M. P. Martins and A. Rossi, *J. Fungi*, 2021, **7**, 629.

26 A. Chakrabarti and M. Sharma, *Curr. Fungal Infect. Rep.*, 2019, **13**, 1–10.

27 S. Thakur and N. Karak, *Carbon N. Y.*, 2012, **50**, 5331–5339.

28 M. P. Lavin-Lopez, A. Paton-Carrero, L. Sanchez-Silva, J. L. Valverde and A. Romero, *Adv. Powder Technol.*, 2017, **28**, 3195–3203.

29 M. Sedki, M. B. Mohamed, M. Fawzy, D. A. Abdelrehim and M. M. S. A. Abdel-Mottaleb, *RSC Adv.*, 2015, **5**, 17358–17365.

30 L. Chen, Z. Li and M. Chen, *J. Environ. Chem. Eng.*, 2019, **7**, 103160.

31 S. Zhou, H. Ji, Y. Fu, Y. Yang and C. Lü, *Appl. Surf. Sci.*, 2020, **506**, 144655.

32 S. Bhattacharjee, R. Joshi, M. Yasir, A. Adhikari, A. A. Chughtai, D. Heslop, R. Bull, M. Willcox and C. R. Macintyre, *ACS Appl. Bio Mater.*, 2021, **4**, 6175–6185.

33 M. Sawangphruk, P. Srimuk, P. Chiochan, T. Sangsri and P. Siwayaprahm, *Carbon N. Y.*, 2012, **50**, 5156–5161.

34 O. Akhavan and E. Ghaderi, *ACS Nano*, 2010, **4**, 5731–5736.

35 F. Perreault, A. F. de Faria, S. Nejati and M. Elimelech, *ACS Nano*, 2015, **9**, 7226–7236.

36 B. Gottardo, T. H. Lemes, G. Byzynski, M. H. Paziani, M. R. Von-Zeska-Kress, M. T. G. de Almeida and D. P. Volanti, *ACS Appl. Nano Mater.*, 2019, **2**, 2112–2120.

37 S. J. Taj-Aldeen, H. Salah, A. M. S. Al-Hatmi, M. Hamed, B. Theelen, A. D. van Diepeningen, T. Boekhout and C. Lass-Flörl, *Diagn. Microbiol. Infect. Dis.*, 2016, **85**, 438–443.

38 K.-J. Kim, W. S. Sung, B. K. Suh, S.-K. Moon, J.-S. Choi, J. G. Kim and D. G. Lee, *BioMetals*, 2009, **22**, 235–242.

39 T. Mochizuki, R. Tsuboi, K. Iozumi, S. Ishizaki, T. Ushigami, Y. Ogawa, T. Kaneko, M. Kawai, Y. Kitami, M. Kusuhara, T. Kono, T. Sato, T. Sato, H. Shimoyama, M. Takenaka, H. Tanabe, G. Tsuji, Y. Tsunemi, Y. Hata, K. Harada, T. Fukuda, T.

Matsuda and R. Maruyama, *J. Dermatol.*, 2020, **47**, 1343–1373.

40 N. Teixera De Aguiar Peres, F. Cristina, A. Maranhão, A. Rossi and N. Maria Martinez-Rossi, *An Bras Dermatol*, 2010, **85**, 657–67.

41 K. C, S. N, P. P. S and C. DG, *J. Environ. Chem. Eng.*, 2020, **8**, 103577.

42 X.-Z. Tang, X. Chen, G. Wu, X. Hu and J. Yang, *RSC Adv.*, 2015, **5**, 49257–49262.

43 A. M. El Badawy, T. P. Luxton, R. G. Silva, K. G. Scheckel, M. T. Suidan and T. M. Tolaymat, *Environ. Sci. Technol.*, 2010, **44**, 1260–1266.

44 C. Xu, X. Wang and J. Zhu, *J. Phys. Chem. C*, 2008, **112**, 19841–19845.

45 R. D. de Castro and E. O. Lima, *Brazilian Arch. Biol. Technol.*, 2013, **56**, 749–755.

46 K. A. Qureshi, M. Imtiaz, A. Parvez, P. K. Rai, M. Jaremko, A.-H. Emwas, A. D. Bholay and M. Q. Fatmi, *Antibiotics*, 2022, **11**, 79.

47 R. Rani, D. Sharma, M. Chaturvedi and J. Parkash Yadav, *Clin. Microbiol. Open Access*, , DOI:10.4172/2327-5073.1000280.

48 A. Mancy, *Our Dermatology Online*, 2022, **13**, 36–40.

49 D. Gu, X. Chang, X. Zhai, S. Sun, Z. Li, T. Liu, L. Dong and Y. Yin, *Ceram. Int.*, 2016, **42**, 9769–9778.

50 J. Chen, H. Peng, X. Wang, F. Shao, Z. Yuan and H. Han, *Nanoscale*, 2014, **6**, 1879–1889.

51 D. Kichukova, D. Kovacheva, A. Staneva and I. Spassova, *Antimicrobial Impact of Nanocomposites of Reduced Graphene Oxide with Silver and Copper*, 2021, vol. 74.

52 B. Kably, M. Launay, A. Derobertmasure, S. Lefeuvre, E. Dannaoui and E. M. Billaud, *Ther. Drug Monit.*, 2022, **44**, 166–197.

53 T. Pereira, P. de Barros, L. Fugisaki, R. Rossoni, F. Ribeiro, R. de Menezes, J. Junqueira and L. Scorzoni, *J. Fungi*, 2018, **4**, 128.

54 K. Ignasiak and A. Maxwell, *BMC Res. Notes*, 2017, **10**, 428.

55 S. Azarmi, W. H. Roa and R. Löbenberg, *Adv. Drug Deliv. Rev.*, 2008, **60**, 863–875.

56 CLSI, *Clinical and Laboratory Standards Institute: Método de Referência para Testes de Diluição em Caldo para a Determinação da Sensibilidade a Terapia Antifúngica das Leveduras*, 2002, vol. 22.

57 Clinical and Laboratory Standards Institute (CLSI), *Ref. method broth dilution Antifung. susceptibility Test. yeasts. Approv. Stand. 3th ed.*, 2008, **28**, 0–13.

58 M. E. Klepser, E. J. Wolfe and M. A. Pfaller, *J. Antimicrob. Chemother.*, 1998, **41**, 397–401.

59 I. Bernardes, M. P. Felipe Rodrigues, G. K. Bacelli, E. Munin, L. P. Alves and M. S.

Costa, *Mycoses*, 2012, **55**, 257–261.

60 M. H. Paziani, L. Tonani, H. D. de Menezes, L. Bachmann, M. Wainwright, G. Ú. L. Braga and M. R. von Zeska Kress, *Photodiagnosis Photodyn. Ther.*, 2019, **25**, 197–203.

5 CONCLUSÕES

Este estudo mostra uma síntese de nanocompósitos híbridos contendo uma matrix atóxica sendo representado por óxido de grafeno reduzido, e por um agente fungicida, a prata nanoparticularizada (Ag NPs). Assim sendo, os nanocompósitos apresentam prata nanoestruturada esférica entre 5-30nm sob malha de óxido de grafeno reduzido, demostrado pelas análises de microscopia eletrônica e DRX.

O híbrido rGO/Ag foi testado contra isolados clínicos apresentando ação antifúngica sinérgica: CIM 3.9 e 1.9 µg/mL.

Curiosamente, o notável desempenho antifúngico mostrado pelos NCs pode ser atribuído à força de interaçãodo rGO/Ag com superfície da parede celular fúngica, com especificidade para alguns receptores, demostrado pelo teste de microdiluição com suplementação de sorbitol a 0.8M. Além disso, as estruturas fúngicas apresentaram interferência a partir de 2 horas e 12 horas para as leveduras e dermatófitos, respectivamente. As leveduras tiveram inibição na formação de hifas, e os dermatófitos reduziram o tamanho do diâmetro das colônias. O efeito não tóxico in vivo pode ser devido a dispersão homogênea de Ag NPs na matriz de malhas do rGO, que protegem o hospedeiro contra danos celulares, apresentado pelo teste *in vivo* de *Galleria mellonella*.

Os achados contribuem para novas perspectivas terapêuticas para o controle de doenças fúngicas superficiais especialmente devido o amplo espectro de atividades dos materiais nanoparticularizados, como biocompatibilidade e baixa toxicidade.

REFERÊNCIAS DA INTRODUÇÃO

AĞBULUT, Ümit *et al.* Synthesis of graphene oxide nanoparticles and the influences of their usage as fuel additives on CI engine behaviors. *Energy*, v. 244, p. 122603, abr. 2022. Disponível em: <https://linkinghub.elsevier.com/retrieve/pii/S0360544221028528>.

ALIAMRADNI, Vahid; ABOLMAALI, Samira Sadat; BORANDEH, Sedigheh. Antifungal and antibacterial properties of graphene-based nanomaterials: A mini-review. *Journal of Nanostructures*, v. 9, n. 3, p. 402–413, 2019.

BEGUM, Jubeda *et al.* Recent advances in the diagnosis of dermatophytosis. *Journal of Basic Microbiology*, v. 60, n. 4, p. 293–303, abr. 2020. Disponível em: <https://onlinelibrary.wiley.com/doi/10.1002/jobm.201900675>.

BHATTACHARJEE, Shovon *et al.* Graphene- and Nanoparticle-Embedded Antimicrobial and Biocompatible Cotton/Silk Fabrics for Protective Clothing. *ACS Applied Bio Materials*, v. 4, n. 8, p. 6175–6185, 2021.

C, Karthik *et al.* Green synthesized rGO-AgNP hybrid nanocomposite – An effective antibacterial adsorbent for photocatalytic removal of DB-14 dye from aqueous solution. *Journal of Environmental Chemical Engineering*, v. 8, n. 1, p. 103577, fev. 2020. Disponível em: <https://doi.org/10.1016/j.jece.2019.103577>.

CAIRES, Cynthia S.A. *et al.* Effective killing of bacteria under blue-light irradiation promoted by green synthesized silver nanoparticles loaded on reduced graphene oxide sheets. *Materials Science and Engineering: C*, v. 113, n. April, p. 110984, ago. 2020. Disponível em: <https://doi.org/10.1016/j.msec.2020.110984>.

CHARELLI, Letícia Emiliano *et al.* Polymeric nanoparticles as therapeutic agents against coronavirus disease. *Journal of Nanoparticle Research*, v. 24, n. 1, p. 12, 10 jan. 2022. Disponível em: <https://doi.org/10.1007/s11051-022-05396-5>.

CHEN, Juanni *et al.* Graphene Oxide-Silver Nanocomposite: Novel Agricultural

Antifungal Agent against Fusarium graminearum for Crop Disease Prevention. *ACS Applied Materials & Interfaces*, v. 8, n. 36, p. 24057–24070, 14 set. 2016. Disponível em: <https://pubs.acs.org/doi/10.1021/acsami.6b05730>.

CHEN, Long; LI, Zhi; CHEN, Mingguang. Facile production of silver-reduced graphene oxide nanocomposite with highly effective antibacterial performance. *Journal of Environmental Chemical Engineering*, v. 7, n. 3, p. 103160, jun. 2019. Disponível em: <https://doi.org/10.1016/j.jece.2019.103160>.

CHINNAPUN, Dutsadee. Virulence factors involved in pathogenicity of dermatophytes. *Walailak Journal of Science and Technology*, v. 12, n. 7, p. 573–580, 2015.

EL-SONBATY, Sawsan; KANDIL, Eman I.; HAROUN, Riham Abdel-Hamid. Assessment of the Antitumor Activity of Green Biosynthesized Zinc Nanoparticles as Therapeutic Agent Against Renal Cancer in Rats. *Biological Trace Element Research*, n. 0123456789, 26 jan. 2022. Disponível em: <https://doi.org/10.1007/s12011-022-03126-5>.

ELBASUNEY, Sherif *et al.* Promising antimicrobial and antibiofilm activities of reduced graphene oxide-metal oxide (RGO-NiO, RGO-AgO, and RGO-ZnO) nanocomposites. *RSC Advances*, v. 11, n. 42, p. 25961–25975, 2021. Disponível em: <http://xlink.rsc.org/?DOI=D1RA04542C>.

FADIL, Yasemin *et al.* Synthesis of graphene-based polymeric nanocomposites using emulsion techniques. *Progress in Polymer Science*, v. 125, p. 101476, fev. 2022. Disponível em: <https://doi.org/10.1016/j.progpolymsci.2021.101476>.

FENNICHE, F. *et al.* Electrochemical Synthesis of Reduced Graphene Oxide–Wrapped Polyaniline Nanorods for Improved Photocatalytic and Antibacterial Activities. *Journal of Inorganic and Organometallic Polymers and Materials*, v. 32, n. 3, p. 1011–1025, 22 mar. 2022. Disponível em: <https://doi.org/10.1007/s10904-021-02204-w>.

GNAT, S.; ŁAGOWSKI, D.; NOWAKIEWICZ, A. Major challenges and perspectives in the diagnostics and treatment of dermatophyte infections. *Journal of Applied Microbiology*, v. 129, n. 2, p. 212–232, 26 ago. 2020. Disponível em: <https://onlinelibrary.wiley.com/doi/10.1111/jam.14611>.

GRANINGER, Wolfgang; DIAB-ELSCHAHAWI, Magda; PRESTERL, Elisabeth. *Clinically Relevant Mycoses*. Cham: Springer International Publishing, 2019. Disponível em: <http://link.springer.com/10.1007/978-3-319-92300-0>.

GUPTA, Aditya K.; VENKATARAMAN, Maanasa. Antifungal resistance in superficial mycoses. *Journal of Dermatological Treatment*, v. 0, n. 0, p. 1–8, 30 jun. 2021. Disponível em: <https://doi.org/10.1080/09546634.2021.1942421>.

HUMMERS, William S.; OFFEMAN, Richard E. Preparation of Graphitic Oxide. *Journal of the American Chemical Society*, v. 80, n. 6, p. 1339–1339, mar. 1958.

HUQ, Md Amdadul *et al.* Green Synthesis and Potential Antibacterial Applications of Bioactive Silver Nanoparticles: A Review. *Polymers*, v. 14, n. 4, p. 742, 15 fev. 2022. Disponível em: <https://www.mdpi.com/2073-4360/14/4/742>.

IGNASIAK, Katarzyna; MAXWELL, Anthony. Galleria mellonella (greater wax moth) larvae as a model for antibiotic susceptibility testing and acute toxicity trials. *BMC Research Notes*, v. 10, n. 1, p. 428, dez. 2017.

JAWORSKI, Sławomir *et al.* Graphene Oxide-Based Nanocomposites Decorated with Silver Nanoparticles as an Antibacterial Agent. *Nanoscale Research Letters*, v. 13, n. 1, p. 116, 23 dez. 2018. Disponível em: <https://nanoscalereslett.springeropen.com/articles/10.1186/s11671-018-2533-2>.

KABLY, Benjamin *et al.* Antifungal Drugs TDM: Trends and Update. *Therapeutic Drug Monitoring*, v. 44, n. 1, p. 166–197, 1 fev. 2022. Disponível em: <https://journals.lww.com/10.1097/FTD.0000000000000952>. Acesso em: 18 mar. 2022.

KESHVARDOOSTCHOKAMI, Mina *et al.* Fabrication and Antibacterial Properties of Silver/Graphite Oxide/Chitosan and Silver/Reduced Graphene Oxide/Chitosan Nanocomposites. *JOM*, v. 72, n. 12, p. 4477–4485, 12 dez. 2020. Disponível em: <https://doi.org/10.1007/s11837-020-04243-z>.

KOSA, Samia A.; ZAHEER, Zoya. Biogenic fabrication of silver nanoparticles, oxidative dissolution and antimicrobial activities. *Journal of Saudi Chemical Society*, v. 26, n. 1, p. 101414, jan. 2022. Disponível em: <https://doi.org/10.1016/j.jscs.2021.101414>.

KURANTOWICZ, Natalia *et al.* Interaction of graphene family materials with Listeria monocytogenes and Salmonella enterica. *Nanoscale Research Letters*, v. 10, n. 1, p. 23, 28 dez. 2015. Disponível em: <https://nanoscalereslett.springeropen.com/articles/10.1186/s11671-015-0749-y>.

LAVIN-LOPEZ, M.P. *et al.* Influence of the reduction strategy in the synthesis of reduced graphene oxide. *Advanced Powder Technology*, v. 28, n. 12, p. 3195–3203, dez. 2017. Disponível em: <https://doi.org/10.1016/j.apt.2017.09.032>.

LIPNER, Shari R.; SCHER, Richard K. Onychomycosis. *Journal of the American Academy of Dermatology*, v. 80, n. 4, p. 835–851, abr. 2019. Disponível em: <https://linkinghub.elsevier.com/retrieve/pii/S0190962218321881>.

MARTINEZ-ROSSI, Nilce M. *et al.* State-of-the-Art Dermatophyte Infections: Epidemiology Aspects, Pathophysiology, and Resistance Mechanisms. *Journal of Fungi*, v. 7, n. 8, p. 629, 3 ago. 2021. Disponível em: <https://www.mdpi.com/2309-608X/7/8/629>.

MISHRA, Monalisa; PANDA, Mrutyunjaya. Reactive oxygen species: the root cause of nanoparticle-induced toxicity in Drosophila melanogaster. *Free Radical Research*, v. 55, n. 8, p. 919–935, 3 ago. 2021. Disponível em: <https://doi.org/10.1080/10715762.2021.1914335>.

MOCHIZUKI, Takashi *et al.* Guidelines for the management of dermatomycosis

(2019). *The Journal of Dermatology*, v. 47, n. 12, p. 1343–1373, 25 dez. 2020. Disponível em: <https://onlinelibrary.wiley.com/doi/10.1111/1346-8138.15618>.

MOYA-ANDÉRICO, Laura *et al.* Utility of Galleria mellonella larvae for evaluating nanoparticle toxicology. *Chemosphere*, v. 266, p. 129235, mar. 2021. Disponível em: <https://linkinghub.elsevier.com/retrieve/pii/S0045653520334329>.

MUHAJ, Fiorinda F. *et al.* Antimicrobials and Resistance Part II: Antifungals, Antivirals, and Antiparasitics. *Journal of the American Academy of Dermatology*, fev. 2022. Disponível em: <https://doi.org/10.1016/j.jaad.2021.11.065>.

OWAID, Mustafa Nadhim *et al.* Mycogenic fabrication of silver nanoparticles using Picoa, Pezizales, characterization and their antifungal activity. *Environmental Nanotechnology, Monitoring & Management*, v. 17, n. August 2021, p. 100612, maio 2022. Disponível em: <https://doi.org/10.1016/j.enmm.2021.100612>.

PAPPAS, Peter G. *et al.* Invasive candidiasis. *Nature Reviews Disease Primers*, v. 4, p. 1445–1456, 2018.

PARVATHY, Subramanian *et al.* The structural, optical, antimicrobial and anticancer properties of biocompatible astaxanthin coated ZnO and CeO2 nanoparticles. *Materials Letters*, v. 312, n. November 2021, p. 131669, abr. 2022. Disponível em: <https://doi.org/10.1016/j.matlet.2022.131669>.

PAZIANI, Mario Henrique *et al.* Antimicrobial photodynamic therapy with phenothiazinium photosensitizers in non-vertebrate model Galleria mellonella infected with Fusarium keratoplasticum and Fusarium moniliforme. *Photodiagnosis and Photodynamic Therapy*, v. 25, n. October 2018, p. 197–203, mar. 2019. Disponível em: <https://doi.org/10.1016/j.pdpdt.2018.12.010>.

PENSADO-LÓPEZ, Alba *et al.* Zebrafish Models for the Safety and Therapeutic Testing of Nanoparticles with a Focus on Macrophages. *Nanomaterials*, v. 11, n. 7, p. 1784, 9 jul. 2021. Disponível em: <https://www.mdpi.com/2079-4991/11/7/1784>.

PEREIRA, Thais *et al.* Recent Advances in the Use of Galleria mellonella Model to Study Immune Responses against Human Pathogens. *Journal of Fungi*, v. 4, n. 4, p. 128, 27 nov. 2018. Disponível em: <http://www.mdpi.com/2309-608X/4/4/128>.

PERREAULT, François *et al.* Antimicrobial Properties of Graphene Oxide Nanosheets: Why Size Matters. *ACS Nano*, v. 9, n. 7, p. 7226–7236, 28 jul. 2015. Disponível em: <https://pubs.acs.org/doi/10.1021/acsnano.5b02067>.

POZDNYAKOV, Alexander *et al.* Strong Antimicrobial Activity of Highly Stable Nanocomposite Containing AgNPs Based on Water-Soluble Triazole-Sulfonate Copolymer. *Pharmaceutics*, v. 14, n. 1, p. 206, 16 jan. 2022. Disponível em: <https://www.mdpi.com/1999-4923/14/1/206>.

PRASAD, Karthika *et al.* Synergic bactericidal effects of reduced graphene oxide and silver nanoparticles against Gram-positive and Gram-negative bacteria. *Scientific Reports*, v. 7, n. 1, p. 1591, 8 dez. 2017. Disponível em: <http://dx.doi.org/10.1038/s41598-017-01669-5>.

QUINTEROS, M.A. *et al.* Oxidative stress generation of silver nanoparticles in three bacterial genera and its relationship with the antimicrobial activity. *Toxicology in Vitro*, v. 36, p. 216–223, out. 2016. Disponível em: <http://dx.doi.org/10.1016/j.tiv.2016.08.007>.

RIDZUAN, P. M. *et al.* Mini Review on Dermatomycosis. *Journal of Science and Mathematics Letters*, v. 8, n. 1, p. 6–15, 7 nov. 2019. Disponível em: <https://ejournal.upsi.edu.my/index.php/JSML/article/view/2686/2065>.

RODRIGUES, Marcelo Costa *et al.* Resistance of filamental fungi in opportunistic mycoses : literature review Resistência de fungos filamentosos em micoses oportunistas : revisão de literatura. v. 2022, p. 1–10, 2022.

SANTOS, Giselle C.de Oliveira *et al.* Candida infections and therapeutic strategies: Mechanisms of action for traditional and alternative agents. *Frontiers in Microbiology*, v. 9, n. JUL, p. 1–23, 2018.

SCRAVONI, Renan; GRZONA, Esteban. Impact of HIV infection in dermatomycosis . Cases and controls study. n. December, 2021.

SEDKI, Mohammed *et al.* Phytosynthesis of silver–reduced graphene oxide (Ag–RGO) nanocomposite with an enhanced antibacterial effect using Potamogeton pectinatus extract. *RSC Advances*, v. 5, n. 22, p. 17358–17365, 2015. Disponível em: <http://xlink.rsc.org/?DOI=C4RA13117G>.

SENGUPTA, Iman *et al.* Bactericidal effect of graphene oxide and reduced graphene oxide: Influence of shape of bacteria. *Colloid and Interface Science Communications*, v. 28, n. December 2018, p. 60–68, jan. 2019. Disponível em: <https://doi.org/10.1016/j.colcom.2018.12.001>.

VASILEV, Krasimir *et al.* Tunable antibacterial coatings that support mammalian cell growth. *Nano Letters*, v. 10, n. 1, p. 202–207, 2010.

VIET, Pham Van *et al.* Silver nanoparticle loaded TiO 2 nanotubes with high photocatalytic and antibacterial activity synthesized by photoreduction method. *Journal of Photochemistry and Photobiology A: Chemistry*, v. 352, p. 106–112, fev. 2018. Disponível em: <http://dx.doi.org/10.1016/j.jphotochem.2017.10.051>.

WHALEY, Sarah G. *et al.* Azole Antifungal Resistance in Candida albicans and Emerging Non-albicans Candida Species. *Frontiers in Microbiology*, v. 7, n. JAN, p. 1–12, 12 jan. 2017. Disponível em: <http://journal.frontiersin.org/article/10.3389/fmicb.2016.02173/full>.

ZHOU, Shengnan *et al.* Mussel-inspired fabrication of cationic polymer modified rGO supported silver nanoparticles hybrid with robust antibacterial and catalytic reduction performance. *Applied Surface Science*, v. 506, n. November, p. 144655, mar. 2020. Disponível em: <https://doi.org/10.1016/j.apsusc.2019.144655>.

APÊNDICE

Supporting Information

Non-toxic nanocomposite based on silver nanoparticles and reduced graphene oxide against agents of dermatomycosis.

Bianca Gottardo[1]; Tarcísio Perfecto[1]; Andreza Zoccal [1], Taiza Maschio-Lima[1]; Thiago H. Lemes[1]; Mario H. Paziani[3]; Marcia Kress[3]; Margarete T.G. Almeida[2]; Diogo P. Volanti [1].

[1] Institute of Biosciences, Humanities, and Exact Sciences, São Paulo State University (UNESP), 2265 Cristóvão Colombo St., 15054-000, São José do Rio Preto, Brazil

[2] São José do Rio Preto Medical School (FAMERP), 5416 Brigadeiro Faria Lima Ave., 15090-000, São José do Rio Preto, Brazil

[3] School of Pharmaceutical Sciences of Ribeirão Preto, University of São Paulo (USP), Café Ave., 14040-903, Ribeirão Preto, Brazil

Antifungal Susceptibility

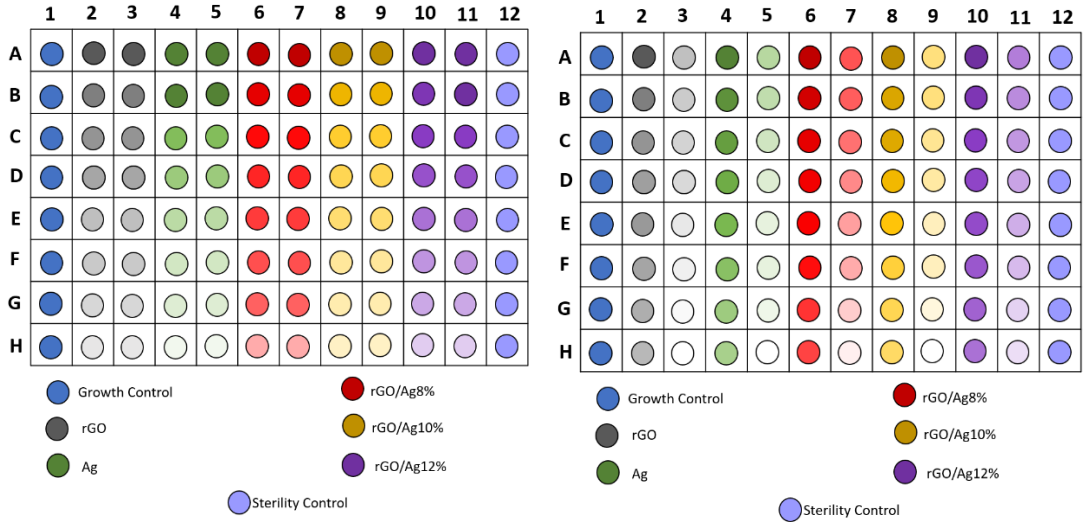

Figure S1: For dermatophyte, the column 1 (A1 to H1 wells) corresponds to growth control; column 2 and 3 (A2 to H2 – A3 to H3 wells), column 4 and 5 (A4 to H4 – A5 to H5 wells), column 6 and 7 (A6 to H6 – A7 to H7 wells), column 8 and 9 (A8 to H8 – A9 to H9 wells), column 10 and 11 (A10 to H10 wells), correspond to serial dilution of NCs; and column 12 (A12 to H12 wells) corresponds to sterility control. at the top-down decreasing concentrations of 250, 125, 62.5, 31.25, 15.62, 7.81, 3.90, and 1.95 $\mu g/mL^{-1}$, in that order. For yeasts the column 1 (A1 to H1 wells) corresponds to growth control. Column 2 (A2 to H2 wells), column4 (A4 to H4 wells), column 6 (A6 to H6 wells), column 8 (A8 to H8 wells), column 10 (A10 to H10 wells), and column 12 (A12 to H12 wells) correspond at the top-down decreasing concentrations of 250, 125, 62.5, 31.25, 15.62, 7.81, 3.90, and 1.95 $\mu g\ mL^{-1}$, in that order. Column 3 (A3 to H3 wells), column 5 (A5 to H5 wells), column 7 (A7 to H7 wells), column 9 (A9 to H9 wells) and column 11 (A11 to H11 wells) correspond to the descending concentrations of NCs top to bottom of 0.9750, 0.4875, 0.24375, 0.121875, 0.0609, 0.03046, 0.015234 and 0.00762 $\mu g\ mL^{-1}$. Source: The autor.

Sorbitol assay

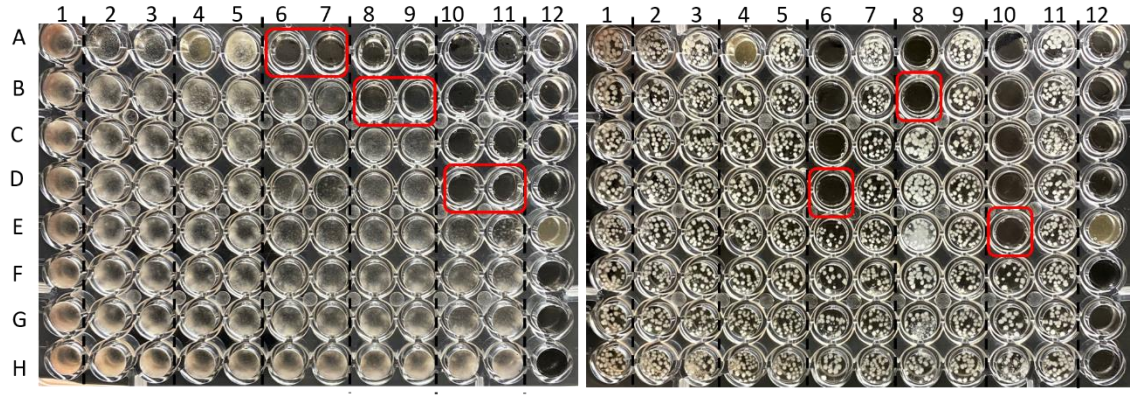

Figure S2: Microdilution test with RPMI supplemented with sorbitol (follow the same preparation in Figure 4), and table, comparing the MIC values with the first non-supplemented test. The increasing MIC value (highlighted by red square), is presented.

Time Kill Assay

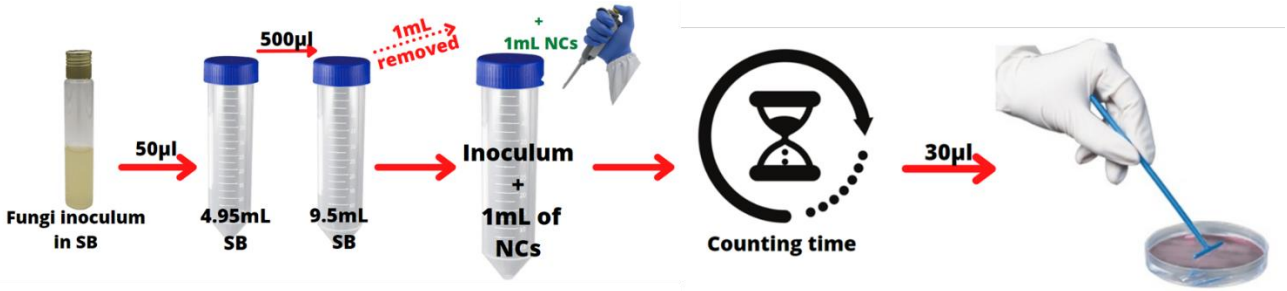

Figure S3: Illustrative scheme of steps to execute the time kill assay. At the first falcon tube, can be observed two types of medium where SB used for yeasts, and PBS, for dermatophytes. Source: The author.

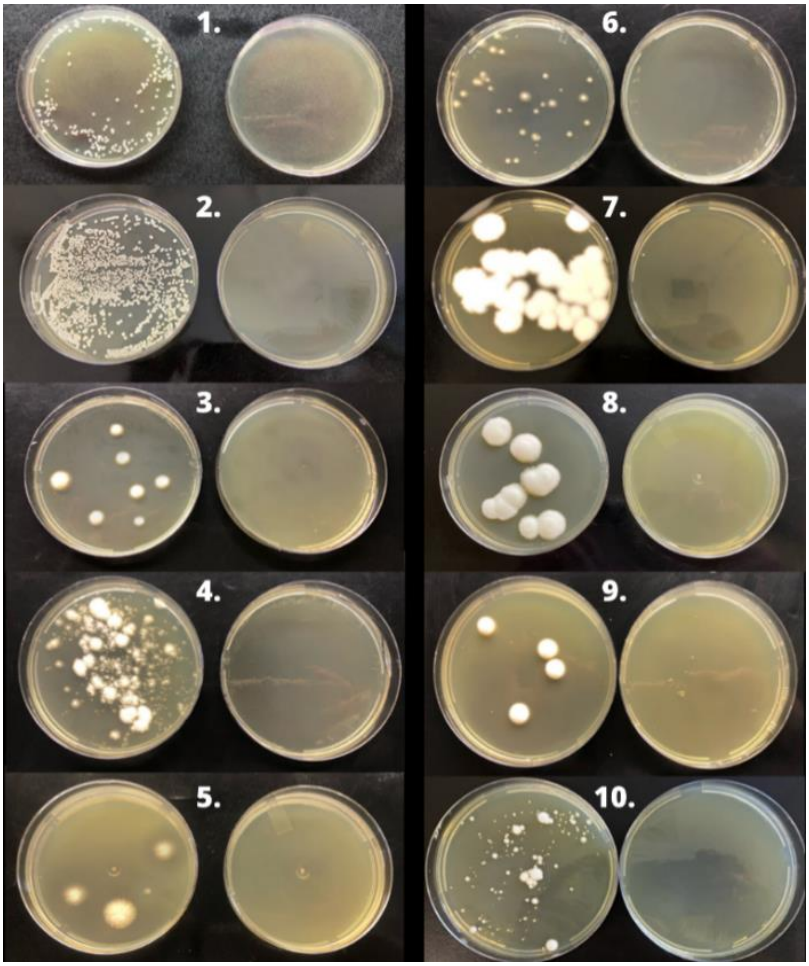

Figure S4: Image of the plates on time kill test presenting the inhibition activity (treated with NCs) in comparison with control culture (on the left). 1) CA1; 2) CP1; 3-4) EF1 and EF2; 5-6) MC1 and MC2; 7-8) TM1 and TM2; 9-10) TR1 and TR2.

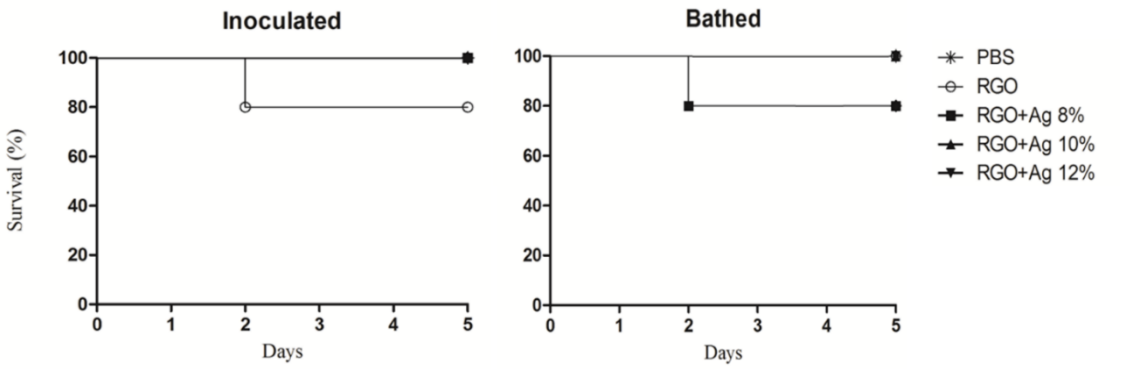

Figure S5: Graphic representation of toxicity test of rGO, rGO/Ag NCs and controls (PBS compound) in *Galleria mellonella* larvae inoculated and bathed ($p<0.05$).